
للتكنولوجيا الاسلامية الجامعة

**UNIVERSITE ISLAMIQUE DE TECHONOLOGIE**

**ISLAMIC UNIVERSITY OF TECHNOLOGY**

**DHAKA, BANGLADESH**

**ORGANIZATION OF ISLAMIC COOPERATION**

# An Investigation of Diaphragm Rupturing Phenomena for Generation of Shock Wave in the Shock Tube

**PREPARED BY**

**SHOHAG HUSSAIN (081417)**

**ISHFAQUE WASEEK (081442)**

**SUPERVISED BY**

**Dr. Mohammad Ali Jinnah**

**Associate Professor, Department of Mechanical and Chemical Engineering**

**Islamic University of Technology (IUT)**

**Organization of Islamic Cooperation (OIC)**

# Declaration

This is to certify that this thesis paper is a unique work on “An investigation of diaphragm rupturing phenomena for generation of shock in the shock tube” .None of its contents are copied or exactly taken from any other researches. The outcome of the research is done by us and neither of this thesis or any part thereof has been submitted anywhere else for the award of any degree or any publication.

**The Author**

# Acknowledgement

First of all we express our heartiest gratefulness to almighty Allah for his countless blessing, which enabled us to complete this thesis successfully. It is our pleasure to express our gratitude to our project supervisor Dr. Mohammad Ali Jinnah, Department Of Mechanical And Chemical Engineering, Islamic University of Technology (IUT) for his constant support, guidance, helpful suggestions and supervision at all stages of this research work. The supervisor had dedicated his valuable time, even at odd hours, which had ensured completion of this project. We also express our sincere gratefulness to Dr. Md. Abdur Razzaq Akhanda. Head of the department, Mechanical and Chemical Engineering (MCE),IUT, for providing us all sorts of support. Special thanks for our beloved parents whose love and inspiration kept us going during this project work.

We are highly indebted to the above-mentioned persons and without their encouragement, it would have been impossible to complete this dissertation.

# Abstract

Shock Wave generation in shock tube now a days very important for Shock Wave study in different fields. For educational purpose the student must visualize what is Shock Wave and it's properties but it is not possible for them to study shock wave outside every time so shock tube is used to study shock tube. On the other hand shock wave is so important for different Chemical study so in laboratory they need shock wave which is only possible by shock tube. In Pharmaceutical field Shock Wave is used very frequently. In medical field Shock Wave becoming very important, in different treatment shock wave is used which was not possible without shock wave. Such as Extracorporeal shock wave lithotripsy (ESWL) is a non-invasive treatment of kidney stones (urinary calculosis) and biliary calculi (stones in the gallbladder or in the liver) using an acoustic pulse. In metallurgy shock wave also used i.e. Shock hardening is a process used to strengthen metals and alloys, wherein a shock wave produces atomic-scale defects in the material's crystalline structure. There are also many applications.

So for creating Shock Wave in shock we must produce supersonic flow in the shock tube. For this the pressure at the driven section must be high enough to create a supersonic air flow. Without high pressure larger MACH number is not possible which is more desirable in shock wave formation. In Shock Tube the Diaphragm is the main element which takes the pressure during shock wave generation, so ***Diaphragm*** should be much stronger to withstand this much pressure in the driven section of the shock tube. If the Diaphragm dose not capable of holding much pressure which is needed to generate shock then the shock tube experiment will be in vain. So for the proper shock wave creation we must select the Diaphragm suitably and also economically.

# Table of Content

**Declaration** 1
**Acknowledgement** 2
**Abstract** 3

***Chapter 1*: Introduction** 8-12

1.1 Introduction 8
1.2 Characteristics 8
1.3 Examples of Shock Wave 9
1.4 Development of Shock Wave 11

***Chapter 2*: Shock wave Propagation in open atmosphere** 13-16

2.1 Introduction 13
2.2 Spherical shock Wave from gun firing 14
2.3 Shockwave from flying Plane with a high speed 15
2.4 Shock wave generated by bursting a balloon 16
2.5 Shock wave formation due to detonation 16

***Chapter 3*: Analysis of compressible flow** 17-22

3.1 Analysis of compressible flow 17
3.2 Effect of Mach number 20
3.3 Relation between the upstream and downstream in terms of the Mach number 20

***Chapter 4*: Numerical Methods** 23-40

4.1 Navier-Stokes Equation 23
4.2 Incompressible flow of Newtonian fluid 25
4.3 Cartesian Coordinates 25
4.4 Conservation of mass 26
4.5 Conservation of linear momentum 28
4.6 Euler Equation 31
4.7 Grid generation with appropriate transformation 33
4.8 Adaptive Grid 35
4.9 Level Multiplier 37
4.10 Tecplot Software 38
4.11 Numerical method used for obtaining Shock wave propagation 39

***Chapter 5*: Determination of Material Properties** 41-51

5.1 Hardness 41
5.2 Hardness Measurement 42
5.3 Tensile Strength and Toughness 46
5.4 Measurement of Tensile Strength and Toughness 48

***Chapter 6*: Generation of Shock Wave in Shock Tube and Measurement of Time 52-58**

6.1 Introduction 52
6.2 Mechanism of Shock Wave generation 55
6.3 Shock Tube 55
6.4 Detailed features of shock tube 57
6.5 Shock tube design consideration 57
6.6 Micro-second level time measuring device 58

***Chapter 7*: Determination if Diaphragm Rupturing Phenomena 66-60**

7.1 Introduction 66
7.2 Diaphragm Material Selection 68
7.3 Measurement of Tensile Strength 69
7.4 Measurement of Hardness 74
7.5 Shock Tube Test 75
7.6 Rupturing Condition of the Diaphragms 79

**Conclusion 82**

**Reference 83**

# List of Figures


| Chapter | Figure no. | Name | Page no. |
|---|---|---|---|
| 1 | 1.1 | Schlieren photograph of supersonic flow over blunt object. Shock wave is detached from object | 9 |
| | 1.2 | Shock wave propagating into a stationary medium, ahead of the fireball of an explosion. The shock is made visible by the shadow effect (Trinity explosion.) | 10 |
| | 1.3 | Shadowgraph of the detached shock on a bullet in supersonic flight, published by Ernst Mach in 1887 | 11 |
| | 1.4 | Travelling of a supersonic body through atmosphere (air) | 12 |
| | 1.5 | Development of shock wave while a supersonic plane is travelling | 12 |
| | | | |
| 2 | 2.1 | Schlieren image of bullet fired from .22 caliber pistol | 14 |
| | 2.2 | Full-scale schlieren image shows the discharge of a .44 Magnum revolver | 15 |
| | 2.3 | Schlieren image of a .30-06 caliber rifle discharge | 15 |
| | 2.4 | F-18 fighter is flying with transonic speed leaving visible signs of shock waves | 15 |
| | 2.5 | Shock Wave is formed due to detonation | 16 |
| | | | |
| 3 | 3.1 | The flow over a cylinder at Re= 19 and M= 0 | 18 |
| | 3.2 | Flow over a cylinder, Re= 140 illustrating the Karman vortex street | 18 |
| | 3.3 | Shadowgraph of a sphere at Mach= 1.7 | 19 |
| | 3.4 | Stationary normal Shock wave in a pipe | 21 |
| | | | |
| 4 | 4.1 | An Airfoil in purely rectangular grid | 35 |
| | 4.2 | Physical Plane and Computational Plane | 35 |
| | 4.3 | Two sketches demonstrating the need to concentrate a number of grid points in the boundary layer. (A) No grid points in the boundary layer. (b) At least some points in the boundary layer. | 36 |
| | 4.4 | Numerical grids of the shock tube and the free space where solid boundaries are for tube and open boundaries are for free space. | 39 |

| | | | |
|---|---|---|---|
| 5 | 5.1 | Rockwell Hardness Tester | 44 |
| | 5.2 | Rockwell Hardness Test Operation | 44 |
| | 5.3 | Universal Material Testing Machine | 48 |
| | 5.4 | Strain vs Stress Curve | 51 |
| | | | |
| 6 | 6.1 | A Shock Tube showing different sections | 55 |
| | 6.2 | Shock Tube used in our experiment | 56 |
| | 6.3 | Micro-second level time measuring device | 59 |
| | 6.4 | Crystal Used in our experiment | 60 |
| | 6.5 | Pin assignment of Motorola MC14518B dual counter | 62 |
| | 6.6 | 7-segments | 63 |
| | 6.7 | Pin assignment of MC14511B BCD to seven segment latch | 65 |
| | 6.8 | Truth table for MC14511B BCD to seven segment latch | 65 |
| | | | |
| | 7.1,2,3 | X-ray film, Rexine ,Celluloid Sheet | 68 |
| | 7.4 | Celluloid Stripes | 69 |
| | 7.5 | Universal Material Testing Machine | 70 |
| | 7.6 | Measurement of Tensile Strength in Universal Material Testing Machine | 70 |
| | 7.7 | Force vs Displacement curve of the X-ray film | 71 |
| | 7.8 | Force vs Displacement curve of the Rexine | 72 |
| | 7.9 | Force vs Displacement curve of the Celluloid Sheet | 73 |
| | 7.10 | Measurement of Hardness Rockwell Hardness Testing Machine | 74 |
| 7 | 7.11 | Shock tube and the position of Triggers | 75 |
| | 7.12 | Fitting of Diaphragm in the Shock Tube | 76 |
| | 7.13 | Diaphragm condition after Shock generation | 77 |
| | 7.14 | Shock Wave generated in our Experiment | 78 |
| | 7.15 | Experimental result obtained in (a) Single- Channeled; (b) Double Channeled micro-second level time measuring | 79 |
| | 7.16 | Condition of X-ray Diaphragm before and after Shock Wave generation | 80 |
| | 7.17 | Condition of Rexine Diaphragm before and after Shock Wave generation | 80 |
| | 7.18 | Condition of Celluloid Sheet Diaphragm before and after Shock Wave generation | 81 |

# Chapter ONE
# Introduction

***Features***

***1.1 Introduction***

***1.2 Characteristics***

***1.3 Examples of Shock Wave***

***1.4 Development of Shock Wave***

## 1.1 Introduction

Shock wave is a compression wave of large amplitude propagating at supersonic velocity, across which stress density, particle velocity, temperature, and related properties change in a nearly discontinuous manner. Unlike acoustic waves, shock waves are characterized by an amplitude dependent velocity. Shock waves arise from sharp and violent disturbances generated from a lightning stroke, bomb blast, or other forms of intense explosion and from steady supersonic flow over bodies.

## 1.2 Characteristics

The abrupt nature of shock wave in a gas can best be visualized from a shadow graph of supersonic flow over objects. Such photograph show well-defined in the flow field across which the density changes rapidly, in contrast to waves within the range of linear dynamic behavior of the fluid. Measurements of fluid density, pressure, and temperature across the surface show that

these quantities always increase in the direction of flow and that the rates of change are usually so rapid as to be beyond the spatial resolution of most instruments These surface of abrupt change of fluid properties are called shock waves or shock fronts.

Shock wave in supersonic flow may be classified as normal or oblique according to whether the orientation of the surface of the abrupt change is perpendicular or at an angle to the direction of flow.

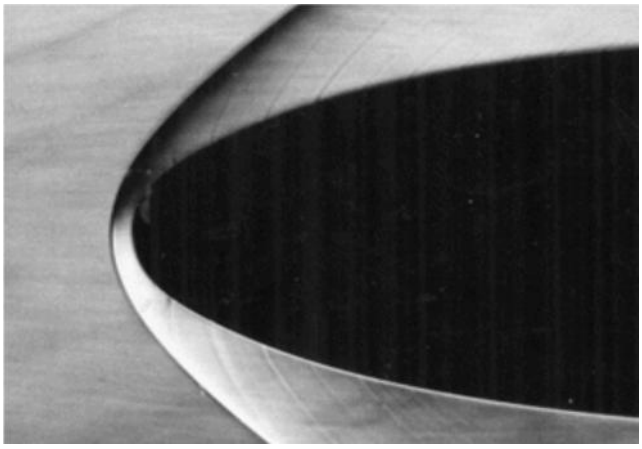

*Figure 1.1: Schlieren photograph of supersonic flow over blunt object. Shock wave is detached from object*

Aschlieren photograph of a supersonic flow over a blunt object is shown in the illustration.

Although this photograph was obtained from a supersonic flow over a stationary model in a shock tube, the general shape of the shock wave around the object is quite typical of those observed in supersonic wind tunnel or of similar objects (or projectiles) flying at supersonic speed in stationary atmosphere. The shock wave in this case assumes an approximately parabolic shape and is clearly detached from the blunt object. The central part of the wave, just in front of the object, may be considered an approximate model of the normal shock; the outer part of the wave is an oblique shock wave of gradually changing obliqueness and strength.

## 1.3 Examples of Shock Wave:

Some common examples of shock waves in condensed material are encountered in the study of underground or underwater explosions, meteorite impacts, and ballistics problems. The field of shock waves in condensed materials (solids or liquids) has grown into an important interdisciplinary area of research involving condensed matter physics geophysics, materials science, applied mechanics, and chemical physics. The nonlinear aspect of shock waves is an important area of applied mathematics.

Experimentally, shock waves are produced by rapidly imparting momentum over a large flat surface. This can be accomplished in many different ways: rapid deposition of radiation using electron or photon beams (lasers or x-rays), detonation of a high explosive in contact with the material, or high-speed impact of a plate on the sample surface. The impacting plate itself can be accelerated by using explosives, electrical discharge, underground nuclear explosions and compressed gases. The use of compressed gas is to accelerate projectiles with appropriate flyer plates provide the highest precision and control as well as convenience in laboratory experiments. Large amplitude one-dimensional compression and shear waves have been studied in solids. In these experiments, a macroscopic volume element is subjected to both a compression and shear deformation. The combined deformation state is produced by impacting two parallel flyer plates that are inclined at an angle to the direction of plate motion. Momentum conservation coupled with different wave velocities for compression and shear waves leads to a separation of these waves in the sample interior. These experiments provide direct information about the shear response of shocked solids, and subject samples to more general loading states than the uniaxial strain state.

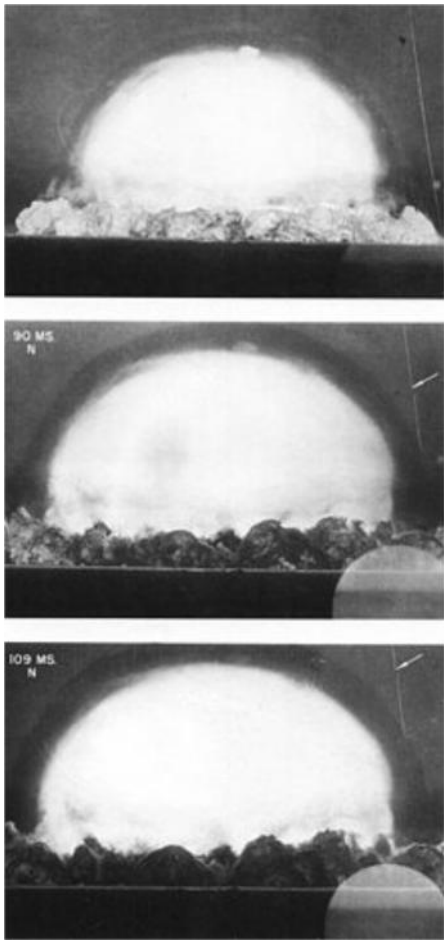


*Figure 1.2: Shock wave propagating into a stationary medium, ahead of the fireball of an explosion. The shock is made visible by the shadow effect (Trinity explosion.)*

Shock wave's subject matter to unusual conditions and therefore provide a good test of understanding of fundamental processes. The majority of the studies on condensed materials have concentrated on mechanical and thermodynamic properties. These are obtained from measurements of shock velocity, stress, and particle velocity in well-controlled experiments. Advanced techniques using electromagnetic gages, laser interferometry, piezoelectric gages and piezo-resistance have been continuous, time-resolved measurements at different sample thickness.

The study of residual effect, that is, the post shock examination of samples subjected to a known pulse amplitude and duration, is of considerable importance to materials science and metallurgy. The conversation of graphite to diamond is noteworthy. Other effects that have been observed are micro structural changes, enhanced chemistry activity, changes in material hardness and strength and changes in electrical and magnetic properties. The generation of shock-induced lattice defects is thought to be important for explaining these changes in material properties. There has been growing interest in using shock methods for material synthesis and powder compaction.

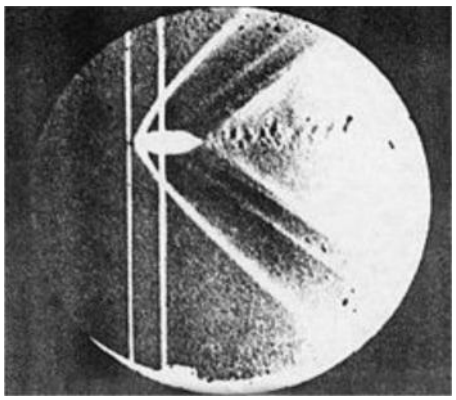

*Figure 1.3: Shadowgraph of the detached shock on a bullet in supersonic flight, published by Ernst Mach in 1887*

## 1.4 Development of shock wave

For some off design values of the pressure ratio in a convergent-divergent nozzle the variation in the fluid properties is sudden and the flow changes from supersonic to subsonic at some sections in the divergent portion; this is due to the formation of "Finite wave fronts" or shock waves at these sections. The thickness of such shock waves is of the order of 10^-3 mm which is comparable with the mean free path of the gas molecules. The following figure shows a constant area which initially contains a gas at rest. Pressure pulses (infinitesimal pressure waves) are transmitted through the gas to the right by the rightward movement of the piston in instantaneous impulses. The growth of one such wave at time t1, t2, t3…… is shown in the figure; the wave travels towards the right with the speed (corresponding to the prevailing temperature) relative to the gas. The portion of the gas which has been traversed by the pressure waves is set in motion. The gas nearer the piston moves at a higher velocity than the gas in the downstream region. On account of this, isentropic expansion of the higher pressure gas on the upstream side occurs continuously towards the lower pressure regions downstream. Thus pressure and temperature gradients along the duct length are established. On account of the higher temperature the speed of the sound is higher in the upstream region. Therefore, the pressure waves in the upstream

region travel at higher velocities on account of higher gas velocity and speed of sound. Thus the upstream waves are continuously overtaking those in the downstream region.

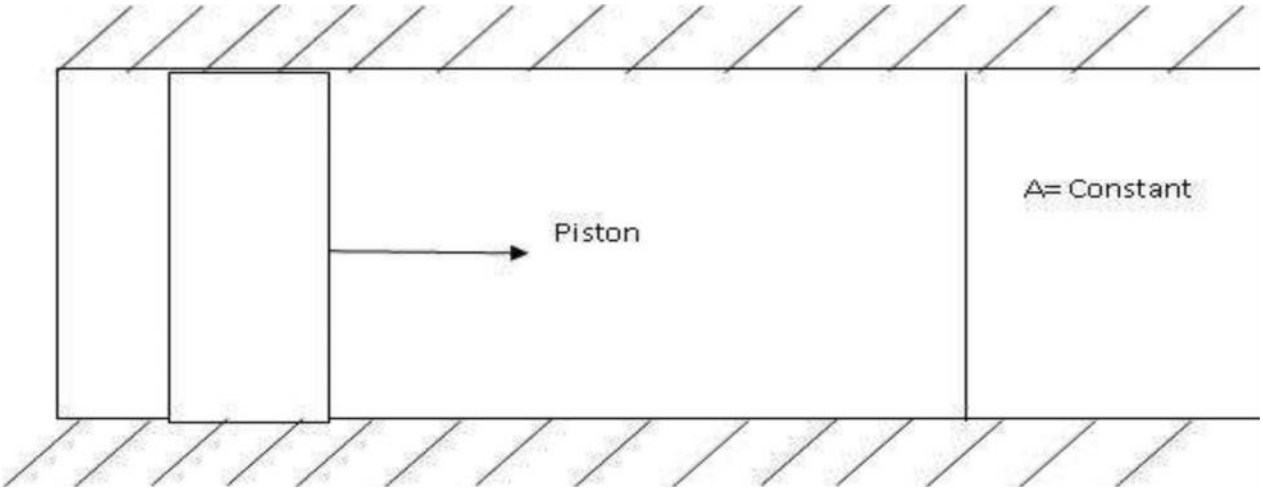


On account of the above phenomena the weak pressure wave generated at time $t=t_1$ grows stronger and steeper as it moves further towards the right. This is due to the other waves overtaking the wave under consideration and consequently strengthens it. If this continuous growth continues, at some stage (as at time t5) it will overturn; this wave form is not possible on account of the impossibility of three different values of pressure occurring simultaneously. Therefore, the extreme form of the wave is vertical. This vertical wave front of finite amplitude is the shock wave across within the changes in pressure, temperature, density; velocity and Mach number are abrupt.

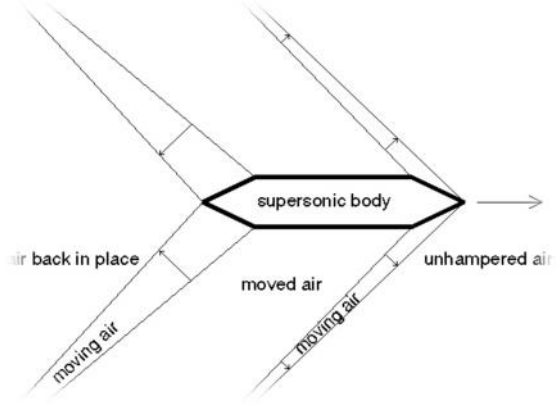


*Figure 1.4: Travelling of a supersonic body through atmosphere (air)*

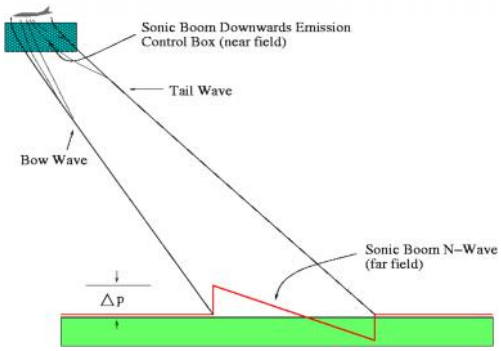


*Figure 1.5: Development of shock wave while a supersonic plane is travelling*

# Chapter TWO
# Shock Wave Propagation in Open Atmosphere

***Features***

***2.1 Introduction***

***2.2 Spherical shock wave from gun firing***

***2.3 Shock wave from flying plane with a high speed***

***2.4 Shock wave generated by bursting a balloon***

***2.5 Shock wave formation due to detonation***

## 2.1 Introduction

When the shock wave propagates in the open atmosphere, as the impulsive wave is generated by the emission of a shock wave from an open end, and unsteady pulse jet is formed near the open end behind the impulsive wave under the specific condition. The pulse jet transits to spherical shock wave with the increase in the strength of shock wave. The strength is dependent on the Mach number of shock wave, relation of shock wave Mach number, distance decay of spherical shock wave and directional characteristics are classified.

## 2.2 Spherical shock wave from gun firing

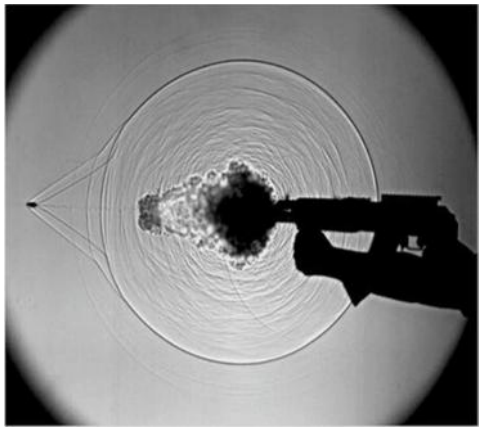

*Figure 2.1: Schlieren image of bullet fired from.22 caliber pistol*

When it comes to firearms, the evolving shock wave of a bullet is rather complicated. First we see the emergence of the bullet-driven shock wave, followed immediately by the bullet itself. Then the propellant gasesthe products of gunpowder combustion exit and expand tremendously as they transfer from the high pressure inside the barrel to the atmosphere outside. These color Schlieren and black & white shadowgraphs technique capture similar information but emphasize complementary details.

The color Schliren photograph captures the firing of a .22-caliber pistol. The air, shockwave and the transonic bullet have left the muzzle, followed by the propellant gases. Toward the right side of the image, thermal convection rises from the gun and the shooter's hand. A frame from high speed shadowgraph video (right) shows the firing of a single round from an AK-47 submachine gun, with its spherical muzzle blast and supersonic bullet trailing oblique shock waves.

The basic optical Schlieren system uses light from a single collimated source shining on a target object. Variations in refractive index caused by density gradients in the fluid distort the collimated beam. This distortion creates a spatial variation in the intensity of the light, which can be visualized directly with a system designed to capture shadows.

.

*Figure 2.2: Full-scale schlieren image shows the discharge of a .44 Magnum revolver*

*Figure2.3: Schlieren image of a .30-06 caliber rifle discharge*

Two spherical shock waves are seen, one centered about the gun's muzzle (the muzzle blast) and a second centered on the cylinder. The supersonic bullet is visible at the far left.

Two pattern shock wave patterns emerge in this high-speed schlieren photograph of a .30-06-caliber rifle discharge. The wake of the supersonic bullet heads to the left. A much larger, spherical shock wave- a phenomenon recently made visible by advanced imaging methods-balloons from the muzzle's length. Hot gases billow from the muzzle's tip.

## 2.3 Shock wave from flying plane with a high speed

U.S. Navy Blue Angel F-18 is flying with transonic speed over the San Francisco Bay leaving visible signs of shockwaves. The air surrounding the plane is first compressed by the shockwaves, as the air suddenly expands, visible moisture condensation is produced. The shockwaves have also induced a wind which is strong enough to leave a small wake on the water.

*Figure 2.4: F-18 fighter is flying with transonic speed leaving visible signs of shock waves*

## 2.4 Shock wave generated by bursting a balloon

Shock wave can be obtained by popping a balloon and releasing the pressurized gas inside. As the gas expands quickly, the surrounding air is pushed out of the way forming shockwaves.

As the balloon bursts, the skin shreds rapidly, revealing a balloon-shaped bubble of compressed air inside. Here, a spherical shock wave is formed despite the initial non spherical shape of the balloon.

## 2.5 Shock wave formation due to detonation:

The detonation of a small 10-milligram silver nitrate charge produces primary and secondary spherical shock waves that are irregular reflected by the ground. In open air shock waves are spherical and symmetrical however, reflection of objects can make the shockwaves complicated.

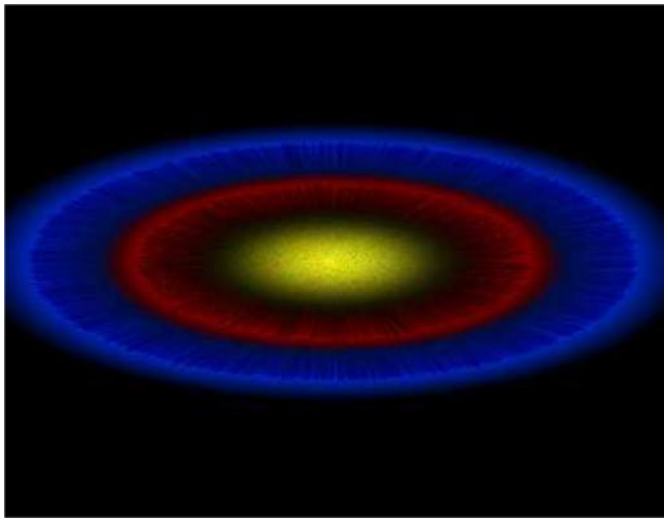

*Figure 2.5: Shock Wave is formed due to detonation*

# Chapter THREE

# Analysis of Compressible Flow

***Features***

***3.1 Analysis of compressible flow***

***3.2 Effect of Mach number***

***3.3 Relation between the upstream & the downstream in terms of the Mach number***

## 3.1 Analysis of compressible flow

The analytical computational solution of the governing equations of fluid dynamics can be a challenging task. Not only are these equations nonlinear but other complicating factors often come into play. Depending on the value of the Reynolds number and other parameters a flow may be steady or unsteady, laminar or turbulent, and incompressible or compressible. In this chapter we focus on finding analytical and computational solutions to the governing equations for incompressible flow.

To construct an analytical solution we must make engineering approximation that simplifies the governing equations to the point that they can be solved. The judgment and decision making skills can be found from the studying the analytical solutions in this chapter are also relevant to using CFD to solve flow problems. Today's computers while extraordinary powerful compared with those available even a few years ago still not able to handle a brute force calculations of the

majority of engineering problems. This is particularly true for turbulent flow for which there are no known analytical solutions. Computational solutions for turbulent flow are based on specialized models whose validity and accuracy are critically dependent on the skill of the person employing the CFD code.

The flow over cylinder changes character as Re increases. The flows at Re=19 and M=0 The flow is also observed to be steady and laminar and since M is small, it is an incompressible flow. At this higher Re, flow separation has occurred resulting in the symmetric vortices and a well defined wake.

Clearly the velocity field is more complex than in creeping flow at lower Reynolds numbers. Since the flow is steady, the local acceleration terms in the Navies-Stokes equations are zero. The convective acceleration terms are not negligible for Re=19, however, and must be retained.

*Figure 3.1: The flow over a cylinder at Re= 19 and M= 0*

The viscous terms in the Nervier-Stokes equations are important in the region close to the cylinder surface 9the boundary layer) and in the wake. There is known analytical solution for a flow at this Re even in an appropriate form. With a further increase in Re vortices are shed and begin to form an oscillating pattern in the wake establishing a structure known as a Karman vortex street.

*Figure 3.2: Flow over a cylinder, Re= 140 illustrating the Karman vortex street*

The flow visualization of streamlines is accomplished by electrolytic precipitation in water. The laminar but unsteady flow, with M negligible, is described by the incompressible continuity and Navier-Stokes equations with no terms neglected. And no analytical solution is available. The unsteady flow over the cylinder causes a periodic lateral force on the cylinder that is important in many applications. In this case, the flow upstream is steady, but the flow over the cylinder is time dependent. Empirical data for this flow are correlated by means of the Reynolds and Strouhal numbers.

At still larger values of Re the boundary layer and wake become turbulent. The Mach number here is still negligible, so the flow is described by the incompressible continuity and Navier-Stokes equations. There are no analytical solutions of the governing equations in the turbulent regime, and using computational fluid dynamics to solve this problem requires the Reynolds equations and a turbulence model.

As the flow speed increases further, it is no longer possible to assume incompressible flow, and the air must be considered to be a compressible fluid. The problem is the described by the continuity, Navier-Stokes, and energy equations.

Figure 3.3 shows the bow shock wave and the wake of a sphere an M=1.7. A shock wave maybe considered being a discontinuity in a continuum flow field; therefore, special techniques are required to treat shock waves analytically or numerically.

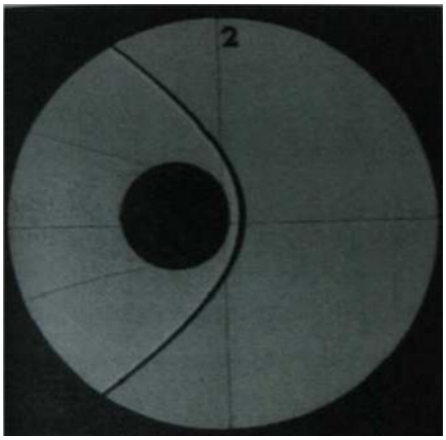


*Figure 3.3: Shadowgraph of a sphere at Mach= 1.7*

## 3.2 Effects of Mach number

The Mach number is the dominant parameter in a compressible flow analysis, with different effects depending upon its magnitude. Aerodynamicists especially make a distinction between the various ranges of Mach number, and the following rough classifications are commonly used.

Ma < 0.3; Incompressible flow, where density effects are negligible.
0.3 <Ma <0.8; Subsonic flow, where density effects are important but no shock waves appear.
0.8 <Ma <1.2; Transonic flow; where shock waves first appear, dividing subsonic and supersonic regions of the flow. Powered flight in the transonic region is difficult because of the mixed character of the flow field.
1.2 <Ma <3.0; Supersonic flow, where shock waves are present but there are no subsonic regions.
3.0 <Ma; Hypersonic flow, where and other flow changes are especially strong.

The numerical values listed above are only rough guides. These five categories of flow are appropriate too external high-speed aerodynamics. For internal (duct) flows, the most important question is simply whether the flow is subsonic (Ma <1) or supersonic (Ma> 1), because the effect of area changes reverses.

## 3.3 Relation between the upstream & the downstream in terms of the Mach number:

As indicated below the various elements of a normal shock wave can be determined by the application of continuity, momentum and energy equations. Considering a stationary normal shock wave developed in a pipe as shown in the figure below. Let,$\rho_u$,$Vu$ and $V_d$, represent the mass density and velocity upstream and downstream of the shock.
Thus according to the continuity equation,

$\rho_U V_u=\rho_d V_d$=G/A (1)

Where G/A is the mass rate of flow per unit area.

$$\rho_U < \rho_d$$


*Figure 3.4: Stationary normal Shock wave in a pipe*

Further if $\rho_U$ and $\rho_d$ are the pressure intensities upstream and downstream of the shock and if the effects of the boundary friction are negligible then applying the momentum equation across the shock, we have,

$(P_u - P_d)\, A = (\text{Mass Flow})\,(V_d - V_u)$

i.e. $P_u - P_d = \rho_d V_d^2 - \rho_U V_u^2$

Or $P_u + \rho_U V_u^2 = P_d + \rho_d V_d^2$ (2)

If it is assumed that there is no heat transfer to or from the pipe, then the energy equation for the flow across the shock maybe obtained as

$$[k/k-1]\,(P_d/\rho_d - P_u/\rho_U) = V_u^2/2 - V_d^2/2 \quad (3)$$

By combining continuity equation (1) and momentum equation (2), we get,

$$P_u + (G/A)^2/\rho_U = P_d + (G/A)^2/\rho_d \quad (4)$$

The above equation is the equation of Rayleigh line.

Similarly by combining the continuity equation (1) and the energy equation (3) we get,

$$(G/A)^2/[2\rho_U 2 + [k/k-1](P_u/\rho_U)] = (G/A)^2/[2\rho_d^2 + [k/k-1](P_d/\rho_d)] \quad (5)$$

The above equation is the equation of the Fanno line.

Further elimination of (G/A) from the above equations (5) & (4) results in the following relationship between the pressure and densities of flow on both sides of a normal shock.

$$P_d/P_u = [(k+1/k-1)\rho_d/\rho_U)-1]/[(k+1/k-1)-(\rho_d/\rho_U)] \quad (6)$$

Or, $\rho_d/\rho_U = V_u/V_d = [1-(k+1/k-1)\ (P_d/P_u]/[(k+1/k-1)+(P_d/P_u)]$ (7)

The above equations (6) &(7) are known as Rankine-Hugoniot equations in honor of W. Rankine and H. Hugoniot who first developed these equations.

Since, velocity is sonic, $C=\sqrt{(pk/\rho)}$ and the Mach number, $Ma=V/C$.

Equations (6) & (7) can be written in alternative form as

$$P_d/P_u = [2k(Ma)u-(k-1)]/(k+1) \quad (8)$$

And $P_d/P_u = V_u/V_d = [(k+1)(Ma)u^2]/[(k-1)(Ma)u^2+2]$ (9)

Where Ma is the Mach number of the upstream of the shock wave. Further by combining the equations 19.50 and 19.51 the following expressions for (Ma)d2, may be obtained

$$(Ma)d^2-[(k^2-1)(Ma)u^2+2]/[2k(Ma)u^2-(k-1)] \quad (10)$$

It may however be noted that as the flow crosses a shock, the energy of flow is conserved, but there is an increase in entropy on the flow process. Therefore the low crossing a shock is irreversible process.

The parameters involved in the equation are:

Ma=Mach no;

P=Pressure;

$\rho$=Density;

K=Adiabatic Exponent=1.40 (for air)

Subscripts u & d stand for upstream & downstream conditions respectively.

# Chapter FOUR
# Numerical Methods

***Features***

***4.1 Navier-Stokes Equation***

***4.2 Incompressible flow of Newtonian fluids***

***4.3 Cartesian coordinates***

***4.4 Conservation of mass***

***4.5 Conservation of linear momentum***

***4.6 Euler Equation***

***4.7 Grid generation with appropriate transformation***

***4.8 Adaptive Grid***

***4.9 Level Multiplier***

***4.10 Tecplot Software***

***4.11 Numerical Method used for obtaining the shock wave propagation***

## 4.1 Navier-Stokes Equation

The Navier–Stokes equations dictate not position but rather velocity. A solution of the Navier–Stokes equations is called a velocity field or flow field, which is a description of the velocity of the fluid at a given point in space and time. Once the velocity field is solved for, other quantities of interest (such as flow rate or drag force) may be found. This is different from what one

normally sees in classical mechanics, where solutions are typically trajectories of position of a particle or deflection of a continuum. Studying velocity instead of position makes more sense for a fluid; however for visualization purposes one can compute various trajectories.

The Navier–Stokes equations are nonlinear partial differential equations in almost every real situation. In some cases, such as one-dimensional flow and Stokes flow (or creeping flow), the equations can be simplified to linear equations. The nonlinearity makes most problems difficult or impossible to solve and is the main contributor to the turbulence that the equations model. The nonlinearity is due to convective acceleration, which is an acceleration associated with the change in velocity over position. Hence, any convective flow, whether turbulent or not, will involve nonlinearity, an example of convective but laminar (non-turbulent) flow would be the passage of a viscous fluid (for example, oil) through a small converging nozzle. Such flows, whether exactly solvable or not, can often be thoroughly studied and understood.

The numerical solution of the Navier–Stokes equations for turbulent flow is extremely difficult, and due to the significantly different mixing-length scales that are involved in turbulent flow, the stable solution of this requires such a fine mesh resolution that the computational time becomes significantly infeasible for calculation (see Direct numerical simulation). Attempts to solve turbulent flow using a laminar solver typically result in a time-unsteady solution, which fails to converge appropriately. To counter this, timeaveraged equations such as the Reynolds-averaged Navier-Stokes equations (RANS), supplemented with turbulence models (such as the k-ε model), are used in practical computational fluid dynamics (CFD) applications when modeling turbulent flows.Another technique for solving numerically the Navier–Stokes equation is the large eddy simulation (LES). This approach is computationally more expensive than the RANS method (in time and computer memory), but produces better results since the larger turbulent scales are explicitly resolved.

The Navier–Stokes equations assume that the fluid being studied is a Continuum not moving at relativistic velocities. At very small scales or under extreme conditions, real fluids made out of discrete molecules will produce results different from the continuous fluids modeled by the Navier-Stokes equations. Depending on the Knudsen number of the problem, statistical mechanics or possibly even molecular dynamics may be a more appropriate approach.

## 4.2 Incompressible flow of Newtonian fluids

A simplification of the resulting flow equations is obtained when considering an incompressible flow of a Newtonian fluid. The assumption of incompressibility rules out the possibility of sound or shock waves to occur; so this simplification is invalid if these phenomena are important. The incompressible flow assumption typically holds well even when dealing with a "compressible" fluid — such as air at room temperature — at low Mach numbers (even when flowing up to about Mach 0.3). Taking the incompressible flow assumption into account and assuming constant viscosity, the Navier–Stokes equations will read, in vector form

$$\rho\frac{D\mathbf{v}}{Dt} = -\nabla p + \nabla\cdot\mathbf{T} + \mathbf{f}.$$

Here f represents "other" body forces (forces per unit volume), such as gravity or centrifugal force. The shear stress term becomes the useful quantity when the fluid is assumed incompressible and Newtonian, where is the dynamic viscosity.

## 4.3 Cartesian coordinates

Writing the vector equation explicitly

$$\rho\left(\frac{\partial u}{\partial t} + u\frac{\partial u}{\partial x} + v\frac{\partial u}{\partial y} + w\frac{\partial u}{\partial z}\right) = -\frac{\partial p}{\partial x} + \mu\left(\frac{\partial^2 u}{\partial x^2} + \frac{\partial^2 u}{\partial y^2} + \frac{\partial^2 u}{\partial z^2}\right) + \rho g_x,$$

$$\rho\left(\frac{\partial v}{\partial t} + u\frac{\partial v}{\partial x} + v\frac{\partial v}{\partial y} + w\frac{\partial v}{\partial z}\right) = -\frac{\partial p}{\partial y} + \mu\left(\frac{\partial^2 v}{\partial x^2} + \frac{\partial^2 v}{\partial y^2} + \frac{\partial^2 v}{\partial z^2}\right) + \rho g_y$$

$$\rho\left(\frac{\partial w}{\partial t} + u\frac{\partial w}{\partial x} + v\frac{\partial w}{\partial y} + w\frac{\partial w}{\partial z}\right) = -\frac{\partial p}{\partial z} + \mu\left(\frac{\partial^2 w}{\partial x^2} + \frac{\partial^2 w}{\partial y^2} + \frac{\partial^2 w}{\partial z^2}\right) + \rho g_z.$$

Note that gravity has been accounted for as a body force, and the values of gx, gy, gz will depend on the orientation of gravity with respect to the chosen set of coordinates.

The continuity equation reads:

$$\frac{\partial \rho}{\partial t} + \frac{\partial (\rho u)}{\partial x} + \frac{\partial (\rho v)}{\partial y} + \frac{\partial (\rho w)}{\partial z} = 0.$$

When the flow is incompressible, does not change for any fluid parcel, and its material derivative vanishes: $D\rho/Dt = 0.$

The continuity equation is reduced to:

$$\frac{\partial u}{\partial x} + \frac{\partial v}{\partial y} + \frac{\partial w}{\partial z} = 0.$$

The velocity components (the dependent variables to be solved for) are typically named u, v, w. This system of four equations comprises the most commonly used and studied form. Though comparatively more compact than other representations, this is still a nonlinear system of partial differential equations for which solutions are difficult to obtain.

## 4.4 Conservation of mass

The law of conservation of mass, also known as principle of mass/matter conservation is that the mass of a closed system (in the sense of a completely isolated system) will remain constant over time. The mass of an isolated system cannot be changed as a result of processes acting inside the system. A similar statement is that mass cannot be created/destroyed, although it may be rearranged in space, and changed into different types of particles. This implies that for any chemical process in a closed system, the mass of the reactants must equal the mass of the products.

As opposed to mass conservation, the principle of matter conservation (in the sense of conservation of particles which are agreed to be "matter") may be considered as an approximate physical law, that is true only in the classical sense, without consideration of special relativity and quantum mechanics. Another difficulty with the idea of conservation of "matter," is that "matter" is not a well-defined word scientifically, and when particles which are considered to be "matter" (such as electrons and positrons) are annihilated to make photons (which are often not considered matter) then conservation of matter does not take place, even in isolated systems.

The general form for a continuity equation is

$$\frac{\partial \varphi}{\partial t} + \nabla . v = \varphi$$

Where

- $\varphi$ is some quantity,
- $\frac{\partial \varphi}{\partial t}$ is the localized storage rate of quantity $\varphi$,
- V is a vector function describing the flow of $\varphi$,
- And describes the generation (or removal if negative) rate of φ

This equation may be derived by considering the flows to an infinitesimal box and the consequences of it flowing in to an infinitesimal box. If $\boldsymbol{\varphi}$ is a conserved quantity, the generation or removal rate is zero:

$$\frac{\partial \varphi}{\partial t} + \nabla . v = 0$$

This general equation may be used to derive any continuity equation, ranging from assimple as the volume continuity equation to as complicated as the Navier-Stokes equations. This equation also generalizes the advection equation.

In electromagnetic theory, the continuity equation can either be regarded as an empirical law expressing (local) charge conservation, or can be derived as a consequence of two of Maxwell's equations. It states that the divergence of the current density is equal to the negative rate of change of the charge density.

$$\nabla . J = -\frac{\partial \rho}{\partial t} .$$

One of Maxwell's equations, Ampere's law, states that

$$\nabla \times H = J + \frac{\partial D}{\partial t}.$$

Taking the divergence of both sides results in

$$\nabla . \nabla \times H = \nabla . J + \frac{\partial \nabla . D}{\partial t}.$$

But the divergence of a curl is zero, so that

$$\nabla \cdot \mathbf{J} + \frac{\partial \nabla \cdot \mathbf{D}}{\partial t} = 0.$$

Another one of Maxwell's equations, Gauss's law, states that

$$\nabla . D = \rho.$$

Substitute this into equation (1) to obtain

$$\nabla . J + \frac{\partial \rho}{\partial t} = 0.$$

This is the continuity equation.

## 4.5 Conservation of linear momentum

The linear momentum of a system of particles can also be defined as the product of the total mass **M** of the system times the velocity of the center of mass $\mathbf{v}_{cm.}$

$$\sum \mathbf{F} = \frac{\mathrm{d}\mathbf{P}}{\mathrm{d}t} = M\frac{\mathrm{d}\mathbf{v}_{cm}}{\mathrm{d}t} = M\mathbf{a}_{cm}$$

This is a special case of Newton's second law. (If mass is constant)

For a more general derivation using tensors, we consider a moving body (see Figure). assumed as a continuum, occupying a volume **V** at a time ***t*** , having a surface area ***S,*** with defined traction or surface forces per unit area represented by the stress vector $T_i^{(n)}$ acting on every point of everybody surface (external and internal), body forces $F_i$ per unit of volume on every point within the volume $V$ , and a velocity field $v_i$ prescribed throughout the body. Following the previous equation, the linear momentum of the system is;

$$\int_S T_i^{(n)} dS + \int_V F_i dV = \frac{d}{dt} \int_V \rho \, v_i \, dV$$

By definition the stress vector is defined as $T_i^{(n)} \equiv \sigma_{ij} n_j$,then

$$\int_S \sigma_{ij} n_j \, dS + \int_V F_i \, dV = \frac{d}{dt} \int_V \rho \, v_i \, dV$$

Using the Gauss's divergence theorem to convert a surface integral to a volume integral gives

$$\int_V \partial_j \sigma_{ij} \, dV + \int_V F_i \, dV = \frac{d}{dt} \int_V \rho \, v_i \, dV$$

Now we only need to take care of the right side of the equation. We have to be careful,
since we cannot just take the differential operator under the integral. This is because while the motion of the continuum body is taking place (the body is not necessarily solid), the volume we are integrating on can change with time too. So the above integral will be:

$$\frac{d}{dt} \int \rho \upsilon dV = \int \frac{\partial(\rho \upsilon)}{\partial t} dV + \oint \rho \upsilon \upsilon n dA$$

Performing the differentiation in the first part, and applying the divergence theorem on the second part we obtain:

$$\frac{d}{dt} \int \rho \, v_i \, dV = \int \left[ \left( \rho \frac{\partial v_i}{\partial t} + v_i \frac{\partial \rho}{\partial t} \right) + \partial_k (\rho v_i v_k) \right] dV$$

Now the second term inside the integral is: $\partial_k(\rho v_i v_k) = \rho v_k \cdot \partial_k v_i + v_i \partial_k(\rho v_k)$

Plugging this into the previous equation, and rearranging the terms, we get:

$$\frac{d}{dt}\int \rho\, v_i \, dV = \int \left[ \left( \rho \frac{\partial v_i}{\partial t} + v_i \frac{\partial \rho}{\partial t} \right) + \partial_k(\rho v_i v_k) \right] dV$$

We can easily recognize the two integral terms in the above equation. The first integral contains the Convective derivative of the velocity vector, and the second integral contains the change and flow of mass in time. Now let's assume that there are no sinks and a source in the system that is mass is conserved, so this term is zero. Hence we obtain:

$$\frac{d}{dt}\int \rho\, v_i \, dV = \int \rho \frac{Dv_i}{Dt} \, dV$$

Putting this back into the original equation:

$$\int_V \left[ \partial_j \sigma_{ij} + F_i - \rho \frac{Dv_i}{Dt} \right] dV = 0$$

For an arbitrary volume the integrand itself must be zero, and we have the Cauchy's equation of motion

$$\partial_j \sigma_{ij} + F_i = \rho \frac{Dv_i}{Dt}$$

As we see the only extra assumption we made is that the system doesn't contain any mass sources or sinks, which means that mass is conserved. So this equation is valid for the motion of any continuum, even for that of fluids. If we are examining elastic continuums only then the second term of the convective derivative operator can be neglected, and we are left with the usual time derivative, of the velocity field.

If a system is in equilibrium, the change in momentum with respect to time is equal to 0, as there is no acceleration. or using

$$\sum \mathbf{F} = \frac{\mathrm{d}\mathbf{P}}{\mathrm{d}t} = M\mathbf{a}_{cm} = 0$$

These are the equilibrium equations which are used in solid mechanics for solving problems of linear elasticity. In engineering notation, the equilibrium equations are expressed in Cartesian coordinates as

$$\frac{\partial \sigma_x}{\partial x} + \frac{\partial \tau_{yx}}{\partial y} + \frac{\partial \tau_{zx}}{\partial z} + F_x = 0$$

$$\frac{\partial \tau_{xy}}{\partial x} + \frac{\partial \sigma_y}{\partial y} + \frac{\partial \tau_{zy}}{\partial z} + F_y = 0$$

$$\frac{\partial \tau_{xz}}{\partial x} + \frac{\partial \tau_{yz}}{\partial y} + \frac{\partial \sigma_z}{\partial z} + F_z = 0$$

## 4.6 Euler Equation:

The Euler equations govern in viscid flow. They correspond to the Navier–Stokes equations with zero viscosity and heat conduction terms. They are usually written in the conservation form shown below to emphasize that they directly represent conservation of mass, momentum, and energy. The Euler equations can be applied to compressible as well as to incompressible flow — using either an appropriate equation of state or assuming that the divergence of the flow velocity field is zero, respectively.

In differential form, the equations are:

$$\frac{\partial \rho}{\partial t} + \nabla \cdot (\rho \mathbf{u}) = 0$$

$$\frac{\partial \rho \mathbf{u}}{\partial t} + \nabla \cdot (\mathbf{u} \otimes (\rho \mathbf{u})) + \nabla p = 0$$

$$\frac{\partial E}{\partial t} + \nabla \cdot (\mathbf{u}(E + p)) = 0,$$

Where

- ρ is the fluid mass density,
- u is the fluid velocity vector, with components u, v, and w,

- $E = \rho e + \frac{1}{2} \rho (u^2 + v^2 + w^2)$ is the total energy per unit volume, with e being the internal energy per unit mass for the fluid, and
- ***p is the pressure.***

The second equation includes the divergence of a dyadic product, and may be clearer in subscript notation, for each j from 1 to 2 one has:

$$\frac{\partial(\rho u_j)}{\partial t} + \sum_{i=1}^{3} \frac{\partial(\rho u_i u_j)}{\partial x_i} + \frac{\partial p}{\partial x_j} = 0,$$

where the i and j subscripts label the three Cartesian components: $(x_1, x_2, x_3) = (x,y,z)$ and $(u_1, u_2, u_3) = (u,v,w)$

Note that the above equations are expressed in conservation form, as this format emphasizes their physical origins (and is often the most convenient form for computational fluid dynamics simulations). The second equation, which represents momentum conservation, can also be expressed in non-conservation form as:

$$\rho \left( \frac{\partial}{\partial t} + \mathbf{u} \cdot \nabla \right) \mathbf{u} + \nabla p = 0$$

But this form obscures the direct connection between the Euler equations and Newton's second law of motion.

## Conservation and vector form

In vector and conservation form, the Euler equations become:

$$\frac{\partial \mathbf{m}}{\partial t} + \frac{\partial \mathbf{f}_x}{\partial x} + \frac{\partial \mathbf{f}_y}{\partial y} + \frac{\partial \mathbf{f}_z}{\partial z} = 0,$$

Where,

$$\mathbf{m} = \begin{pmatrix} \rho \\ \rho u \\ \rho v \\ \rho w \\ E \end{pmatrix};$$

$$\mathbf{f}_x = \begin{pmatrix} \rho u \\ p + \rho u^2 \\ \rho uv \\ \rho uw \\ u(E+p) \end{pmatrix}; \qquad \mathbf{f}_y = \begin{pmatrix} \rho v \\ \rho uv \\ p + \rho v^2 \\ \rho vw \\ v(E+p) \end{pmatrix}; \qquad \mathbf{f}_z = \begin{pmatrix} \rho w \\ \rho uw \\ \rho vw \\ p + \rho w^2 \\ w(E+p) \end{pmatrix}.$$

This form makes it clear that *fx, fy* and *fz* are fluxes.

The equations above thus represent conservation of mass, three components of momentum, and energy. There are thus five equations and six unknowns. Closing the system requires an equation of state; the most commonly used is the ideal gas law (i.e. $p = \rho\,(\gamma - 1)\,e$, where $\rho$ is the density, $\gamma$ is the adiabatic index, and e the internal energy).

Note the odd form for the energy equation; see Rankine–Hugoniot equation. The extra terms involving p may be interpreted as the mechanical work done on a fluid element by its neighbor fluid elements. These terms sum to zero in an incompressible fluid.

The well-known Bernoulli's equation can be derived by integrating Euler's equation along a streamline, under the assumption of constant density and a sufficiently stiff equation of state.

## 4.7 Grid generation with appropriate transformation

The area of grid generation is relatively ‘young’ in practice, although its roots in mathematics are old. This somewhat eclectic area involves the engineer feel for physical behavior, the mathematician understanding of functional behavior, and a lot of imagination, with perhaps a little help from Urania.

The arrangement of discrete points throughout the flow field is simply called grid. The determination of a proper grid for the flow over or through a given geometric shape is a serious matter- one that is by no means trivial. The way that such a grid is determined is called grid generation. The matter of grid generation is a significant consideration in CFD; the type of grid you choose for a given problem can make or break the numerical solution. Because of this grid generation has become an entity by itself in CFD; it is the subject of numerous special conferences, as well as several books.

The generation of an appropriate grid or mesh is one thing; the solution of the governing flow equations over such a grid is quite another thing. The standard finite-difference approach requires a uniform grid. We do not have a direct way of numerically solving the governing flow equations over a non-uniform grid within the context of a finite difference method. Instead the non-uniform grid must (somehow) be transformed into a uniform, rectangular grid. Moreover, along with this transformation, the governing partial differential equations must be recast so as to apply in this transformed, rectangular grid. Since the need for such grid transformation is inherent in the finite difference method, then much of what we have to say in this chapter concerning the transformation of the governing partial equations pertains just to the method.

If all CFD applications dealt with physical problems where a uniform, rectangular grid could be used in the physical plane, there would be no reason to alter the governing partial differential equations. We would siply apply these equations in rectangular *(X, Y, Z, t)* space, finite difference these equations according to the difference quotients derived and calculated away. However, few real problems are ever so accommodating. For example, assume we wish to calculate the flow over an airfoil as skethed in the we have placed the airfoil in a rectangular grid.

1. Some grid points fall inside the airfoil, where they are completely out of the flow. What values of the flow properties do we ascribe to these points?
2. There are few, if any, grid points that fall on the surface of the airfoil, this is not good, because the airfoil surface is a vital boundary condition for the determination of flow, and hence the airfoil surface must be clearly and strongly seen by the numerical solution.

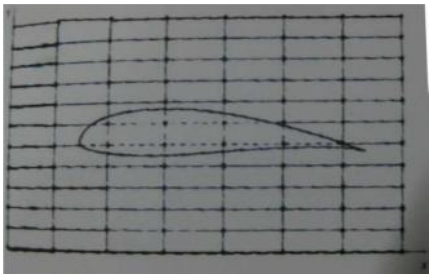

*Figure 4.1: An Airfoil in purely rectangular grid*

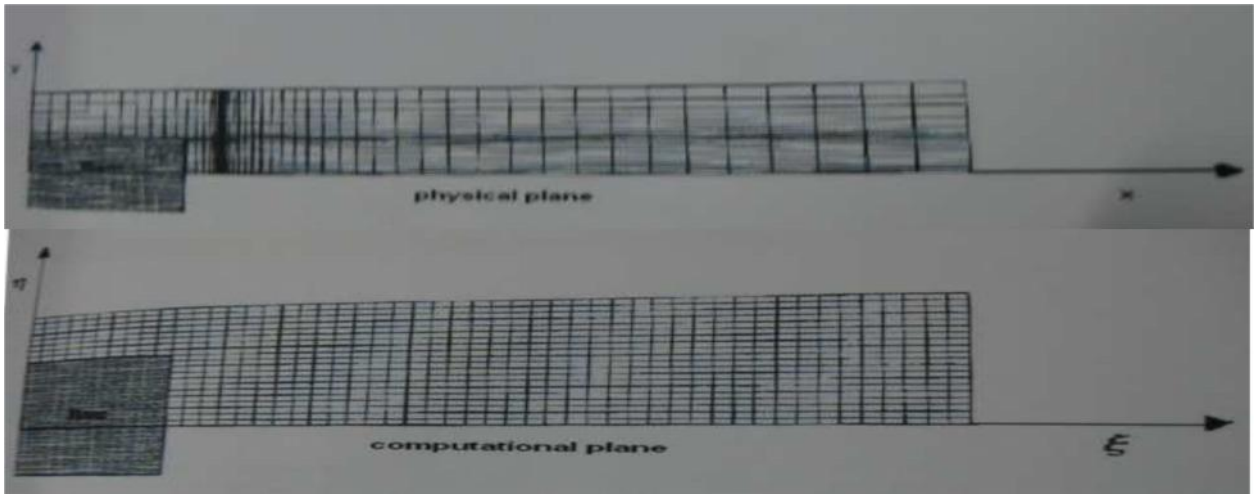


*Figure 4.2: Physical Plane and Computational Plane*

## 4.8 Adaptive Grid

The concept of a stretched grid is motivated by the desire to cluster a large number of closely spaced grid points in those regions of the flow where large gradients in the flow field properties exist, hence improving the numerical accuracy off a given CFD calculation. This motivation is driven by more than just trying to minimize the truncation error with closely spaced points. It is also a matter of simply having enough grid points to properly capture the physics of the flow. A qualitative example of this is due to viscous flow over a plate sketched in the figure next page:

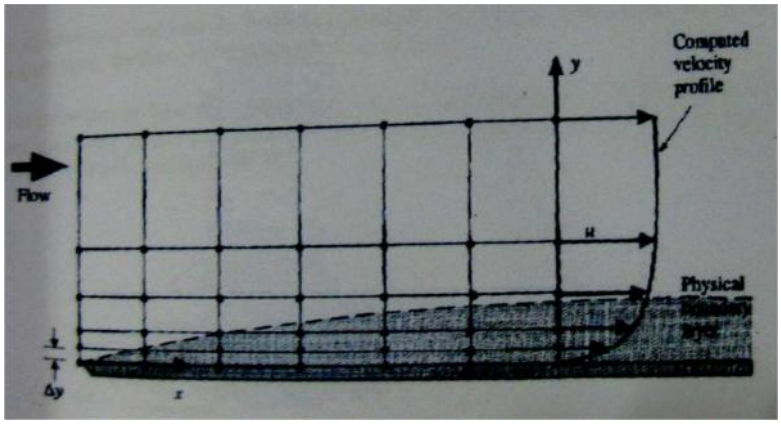


(a)

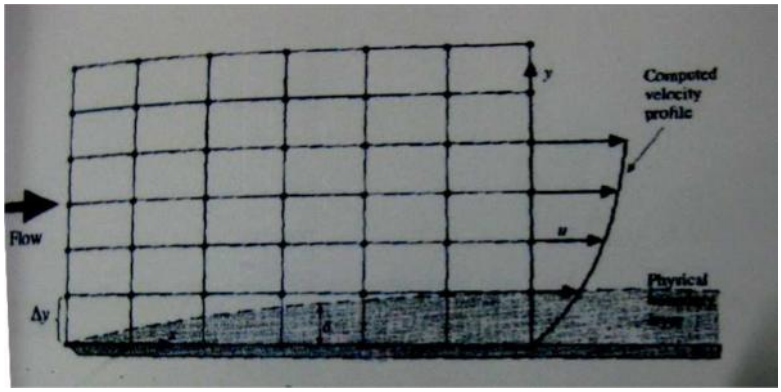


(b)

*Figure 4.3: Two sketches demonstrating the need to concentrate a number of grid points in the boundary layer.(a)no grid points in the boundary layer.(b)at least some points in the boundary layer.*

## 4.9 Level Multiplier

In level multiplier procedure, the cells are selected for refinement in which every cell is divided into new sub cells and these new sub cells are arranged in a particular sequence so that the sub cells are used suitably in the data structure. In three dimensional adaptations the volume of the new sub cell is 1/8 of primary cell, where in two dimensional this fration is 1/8. To avoid unlimited cell refinement around shock wave, either the maximum level of refinement or the minimum cell volume or both are prescribed. When either the level or volume of cell reaches the given limit, further refinement is prohibited.

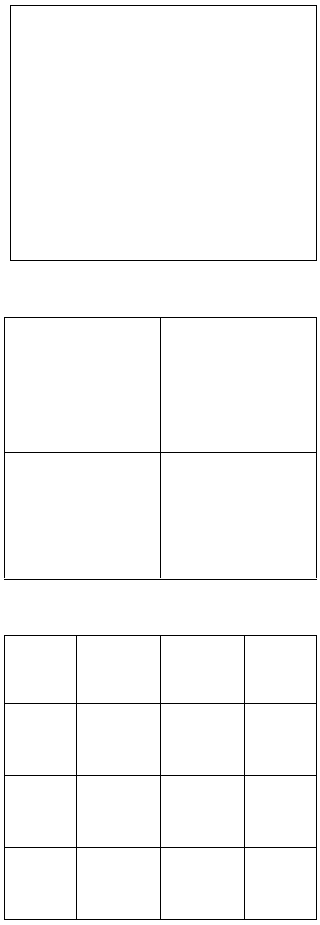

This technique is like the genetical chain, for example a father four sons and these sons again have four sons each, and so total 16 and level of multiplier is four as we can see in the two dimensional level multiplication. A computer program e.g. Fortran, C has been used to generate

sub cell division. Looping has been developed for level multiplication method.The looping is connected to TECPLOT software to simulate the result.

## 4.10 TECPLOT Software

Tecplot 360 is CFD & Numerical Simulation Visualization Software. It combines vital engineering plotting with advanced data visualization in one tool.

With one tool you can:

- Analyze and explore complex datasets
- Arrange multiple XY, 2- and 3-D plots
- Create animations
- Communicate your results with brilliant, high-quality output.

Unlike our competition, Tecplot 360's full range of *XY, 2-D*, and *3- D* capabilities, multiframe workspace, and high-quality output gives you total control to get all the types of plots you want for effective analysis, presentation, and publication.

It's faster: Load on Demand and Parallel Processing.
Smarter loading of data results in faster time to first image and ability to open files that were previously not possible. Load on demand loads just the data you are actively using. For example, a Temperature contour plot only loads *X, Y, Z* and Temperature. When you switch to a new variable to contour (i.e., Pressure), Tecplot loads Pressure and unloads Temperature if needed (assuming it is not being used for anything else). With previous versions, all data needed to be loaded into available memory.

Dual processor Linux and Windows boxes are becoming a standard for desktop engineering workstations. Prior to Tecplot 360, Tecplot was single-threaded and not able to exploit systems maximum resources since all computations were performed by a single CPU. With Tecplot 360 intensive computing operations are spread across all available CPU's leading to faster stream traces, slices, and iso-surfaces.

## 4.11 Numerical Method used for obtaining the shock wave propagation

The two-dimensional Euler equations are solved for the shock wave propagation in the free atmosphere. The governing equation is,

$$\frac{\partial Q}{\partial t}+\frac{\partial F}{\partial x}+\frac{\partial G}{\partial y}=0$$

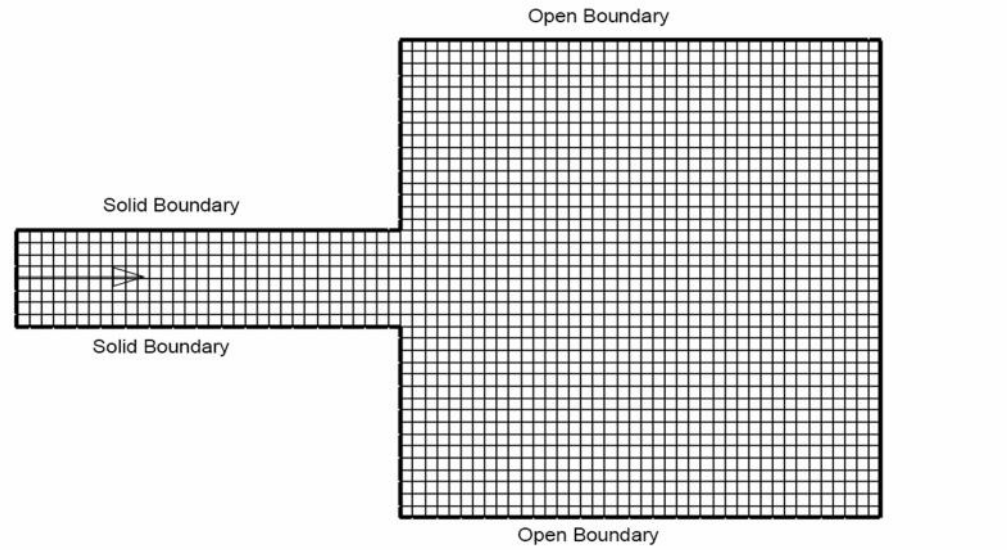


*Figure 4.4: Numerical grids of the shock tube and the free space where solid boundaries are for tube and open boundaries are for free space.*

where Q is the vector of conservative variables, t is the time, F and G are the inviscid flux vectors. The governing equation described above for compressible inviscous flow is discretised by the finite volume method. A second order, upwind Godounov scheme of Flux vector splitting method is used to discrete the inviscid flux terms where HLL-Reimann solver is used for shock capturing in the flow. Two dimensional cells with adaptive grid systems are used for these computations. In this grid systems, the cell-edge data structures are arranged in such a way that each cell contains four faces which are sequence in one to four and each face indicates two neighboring cell that is left cell and right cell providing all faces of a cell are vectorized by

position and coordinate in the grid systems. The initial two-dimensional grid systems are shown in Fig.4.4.

The physical size of each cell before adaptation is equal to 13 x 13 (mm). The grid adaptation is one of the improved and computational time saving techniques, which is used in these computations. The grid adaptation is performed by two procedures, one is refinement procedure and another is coarsening procedure. The refinement and coarsening operations are handled separately in computation. The upstream of incident shock wave is set as inflow boundary condition, the properties and velocities of which are calculated from Rankine- Hugoniot conditions with incident shock Mach number. The downstream inflow boundary conditions are shown in Fig.6.4 and the shock tube wall surface are used as solid boundary conditions where the gradients normal to the surface are taken zero.

# Chapter FIVE
# Determination of Material Properties

*Features*

*5.1 Hardness*

*5.2 Hardness Measurement*

*5.3 Tensile Strength and Toughness*

*5.4 Measurement of Tensile Strength and Toughness*

## 5.1 Hardness

Hardness is the resistance of a material to localized deformation. The term can apply to deformation from indentation, scratching, cutting or bending. In metals, ceramics and most polymers, the deformation considered is plastic deformation of the surface. For elastomers and some polymers, hardness is defined at the resistance to elastic deformation of the surface. The lack of a fundamental definition indicates that hardness is not be a basic property of a material, but rather a composite one with contributions from the yield strength, work hardening, true tensile strength, modulus, and others factors. Hardness measurements are widely used for the

quality control of materials because they are quick and considered to be nondestructive tests when the marks or indentations produced by the test are in low stress areas.

## 5.2Hardness Measurement

Hardness measurement can be defined as macro-, micro- or nano- scale according to the forces applied and displacements obtained.

Measurement of the macro-hardness of materials is a quick and simple method of obtaining mechanical property data for the bulk material from a small sample. It is also widely used for the quality control of surface treatments processes. However, when concerned with coatings and surface properties of importance to friction and wear processes for instance, the macro-indentation depth would be too large relative to the surface-scale features.

Micro hardness is the hardness of a material as determined by forcing an indenter such as a Vickers or Knoop indenter into the surface of the material under 15 to 1000 gf load; usually, the indentations are so small that they must be measured with a microscope. Capable of determining hardness of different microconstituents within a structure, or measuring steep hardness gradients such as those encountered in casehardening. Conversions from micro hardness values to tensile strength and other hardness scales (e.g. Rockwell) are available for many materials.

Micro-indenters works by pressing a tip into a sample and continuously measuring: applied load, penetration depth and cycle time.

### 5.2.1 Different Types of Hardness Measurement

There are a large variety of methods used for determining the hardness of a substance. A few of the more common methods are introduced below.

- Rockwell Hardness Test
- Rockwell Superficial Hardness Test
- Brinell Hardness Test
- Vickers Hardness Test

- Microhardness Test
- Mohs Hardness Test
- Scleroscope and Other Hardness Testing Methods

### 5.2.2 Rockwell Hardness Test

The hardness testing of plastics is most commonly measured by the Rockwell hardness test or Shore (Durometer) hardness test. Both methods measure the resistance of the plastic toward indentation. Both scales provide an empirical hardness value that doesn't correlate to other properties or fundamental characteristics. Rockwell hardness is generally chosen for 'harder' plastics such as nylon, polycarbonate, polystyrene, and acetal where the resiliency or creep of the polymer is less likely to affect the results.

The results obtained from this test are a useful measure of relative resistance to indentation of various grades of plastics. However, the Rockwell hardness test does not serve well as a predictor of other properties such as strength or resistance to scratches, abrasion, or wear, and should not be used alone for product design specifications.

The Rockwell test is a hardness test based on the indentation hardness of a material. The Rockwell test determines the hardness by measuring the depth of penetration of an indenter under a large load compared to the penetration made by a preload. There are different scales, denoted by a single letter, that use different loads or indenters. The result is a dimensionless number noted as HRA, where A is the scale letter.

### 5.2.3 Rockwell Hardness Test Operation

The determination of the Rockwell hardness of a material involves the application of a minor load followed by a major load, and then noting the depth of penetration, vis a vis, hardness value directly from a dial, in which a harder material gives a higher number. The chief advantage of Rockwell hardness is its ability to display hardness values directly, thus obviating tedious calculations involved in other hardness measurement techniques.

The Rockwell hardness number represents the additional depth to which a test ball or sphero-conical penetrator is driven by a heavy (major) load beyond the depth of a previously applied light (minor) load. High hardness numbers that are obtained from hard materials indicate a shallow indentation while low numbers found with soft materials indicate deep indentation. The increment of penetration depth for each point of hardness on the Rockwell scale is 0.00008 inch. For example, if a piece of steel measures Rockwell C 58 (extremely hard) at same point and C 55 at another, the depth of penetration would have been 0.00024 inch deeper at the softer spot.


*Figure 5.1: Rockwell Hardness Tester*

Hardness is not an absolute measurement and hardness can only be compared when the penetrators, loads, and types of materials tested are the same. Several scales are available to the metallurgist. A major load of 150 kg and sphero-conical brace penetrator is used for the C scale for example. This scale is most convenient in testing heat treated and hardened steels. For the C scale, hardness numbers are indicated on the black figured scale of the dial of the analog hardness tester.

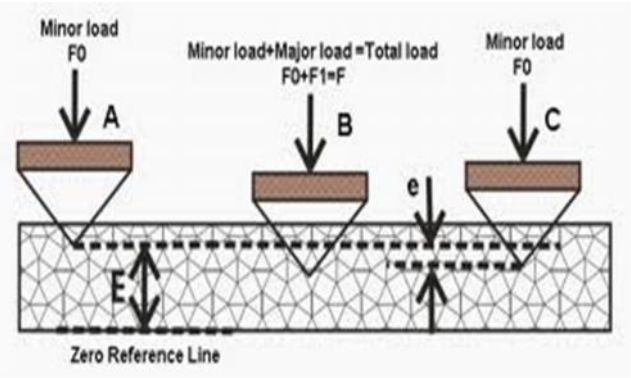


***Figure 5.2: Rockwell Hardness Test Operation***

### 5.2.4 Scales and values

For soft materials such as copper alloys, soft steel, and aluminum alloys a 1/16" diameter steel ball is used with a 100-kilogram load and the hardness is read on the "B" scale. In testing harder materials, hard cast iron and many steel alloys, a 120 degrees diamond cone is used with up to a 150 kilogram load and the hardness is read on the "C" scale. The Rockwell test uses two loads, one applied directly after the other. The first load, known as the "minor", load of 10 kilograms is applied to the specimen to help seat the indenter and remove the effects, in the test, of any surface irregularities. In essence, the minor load creates a uniformly shaped surface for the major load to be applied to. The difference in the depth of the indentation between the minor and major loads provides the Rockwell hardness number. There are several Rockwell scales other than the "B" & "C" scales, (which are called the common scales). The other scales also use a letter for the scale symbol prefix, and many use a different sized steel ball indenter. A properly used Rockwell designation will have the hardness number followed by "HR" (Hardness Rockwell), which will be followed by another letter which indicates the specific Rockwell scale. An example is 60 HRB, which indicates that the specimen has a hardness reading of 60 on the B scale. There is a second Rockwell tester referred to as the "Rockwell Superficial Hardness Tester". This machine works the same as the standard Rockwell tester, but is used to test thin strip, or lightly carburized surfaces, small parts or parts that might collapse under the conditions of the regular test

| Scale | Abbreviation | Load | Indenter | Use |
|---|---|---|---|---|
| A | HRA | 60 kgf | 120° diamond cone | Tungsten carbide |
| B | HRB | 100 kgf | 1/16 inch(1.588 mm) diameter steel sphere | Aluminium, brass and soft materials |
| C | HRC | 150 kgf | 120° diamond cone | Harder materials |
| D | HRD | 100 kgf | 120° diamond cone | |
| E | HRE | 100 kgf | 1/8 inch diameter steel sphere | |
| F | HRF | 60 kgf | 1/16 inch diameter steel sphere | |
| G | HRG | 150 kgf | 1/16 inch diameter steel sphere | |

The *superficial* Rockwell scales use lower loads and shallower impressions on brittle and very thin materials. The 45N scale employs a 45-kgf load on a diamond cone-shaped Brale indenter, and can be used on dense ceramics. The 15T scale employs a 15-kgf load on a $^{1}\!/_{16}$-inch-diameter (1.588 mm) hardened steel ball, and can be used on sheet metal.

## 5.3 Tensile Strength and Toughness

Tensile strength (TS) or ultimate strength, is the maximum stress that a material can withstand while being stretched or pulled before the material breaks or permanently deforms, which is when the specimen's cross-section starts to significantly contract. Tensile strength is the opposite of compressive strength and the values can be quite different.

The UTS is usually found by performing a tensile test and recording the stress versus strain; the highest point of the stress-strain curve is the UTS. It is an intensive property; therefore its value does not depend on the size of the test specimen. However, it is dependent on other factors, such as the preparation of the specimen, the presence or otherwise of surface defects, and the temperature of the test environment and material.

Tensile strengths are rarely used in the design of ductile members, but they are important in brittle members. They are tabulated for common materials such as alloys, composite materials, ceramics, plastics, and wood.

Brittle materials, such as concrete and carbon fiber, are characterized by failure at small strains. They often fail while still behaving in a linear elastic manner, and thus do not have a defined yield point. Because strains are low, there is negligible difference between the engineering stress and the true stress. Testing of several identical specimens will result in different failure stresses, this is due to the Weibull modulus of the brittle material.

The UTS is a common engineering parameter when designing brittle members, because there is no yield point

### 5.3.1 Toughness

In materials science and metallurgy, toughness is the ability of a material to absorb energy and plastically deform without fracturing; Material toughness is defined as the amount of energy per volume that a material can absorb before rupturing. It is also defined as the resistance to fracture of a material when stressed.

Toughness requires a balance of strength and ductility.

### 5.3.2 Mathematical definition

Toughness can be determined by measuring the area (i.e., by taking the integral) underneath the stress-strain curve and its energy of mechanical deformation per unit volume prior to fracture. The explicit mathematical description is:

$$\frac{\text{energy}}{\text{volume}} = \int_0^{\epsilon_f} \sigma \, d\epsilon$$

Where,

$\epsilon$ is strain

$\epsilon_f$ is strain upon failure

$\sigma$ is stress

Another definition is the ability to absorb mechanical (or kinetic) energy up to failure. The area covered under stress strain curve is called toughness.

If the upper limit of integration up to the yield point is restricted, then the energy absorbed per unit volume is known as the modulus of resilience. Mathematically, the modulus of resilience can be expressed by the product of the square of the yield stress divided by two times the Young's modulus.

## 5.4 Measurement of Tensile Strength and Toughness

*Figure5.3: Universal Material Testing Machine*

Mechanical testing plays an important role in evaluating fundamental properties of engineering materials as well as in developing new materials and in controlling the quality of materials for use in design and construction. If a material is to be used as part of an engineering structure that will be subjected to a load, it is important to know that the material is strong enough and rigid enough to withstand the loads that it will experience in service. As a result engineers have developed a number of experimental techniques for mechanical testing of engineering materials subjected to tension, compression, bending or torsion loading. The most common type of test used to measure the mechanical properties of a material is the Tension Test. Tension test is widely used to provide abasic design information on the strength of materials and is an acceptance test for the specification of materials. The major parameters that describe the stress-strain curve obtained during the tension test are the tensile strength (UTS), yield strength or yield point ($\sigma y$), elastic modulus (E), percent elongation ($\Delta L\%$) and the reduction in area (RA%). Toughness, Resilience, Poisson's ratio($\nu$) can also be found by the use of this testing technique.
In this test, a specimen is prepared suitable for gripping into the jaws of the testing machine type that will be used. The specimen used is approximately uniform over a gage length (the length within which elongation measurements are done**).**

Tensile specimens are machined from the material to be tested in the desired orientation and according to the standards. The cross section of the specimen is usually round, square or rectangular. For metals, a piece of sufficient thickness can be obtained so that it can be easily machined, a round specimen is commonly used. For sheet and plate stock, a flat specimen is usually employed.

The change in the gage length of the sample as pulling proceeds is measuredfrom either the change in actuator position (*stroke or overall change in length*) or asensor attached to the sample (*called an extensometer*).

A tensile load is applied to the specimen until it fractures. During the test, the load required to make a certain elongation on the material is recorded. A load elongation curve is plotted by an x-y recorder, so that the tensile behavior of the material can be obtained. An engineering stress-strain curve can be constructed from this load-elongation curve by making the required calculations. Then the mechanical parameters that we search for can be found by studying on this curve. Gage length (**L0**) **do.**

A typical engineering stress-strain diagram and the significant parameters are shown on the figure.
Engineering Stress is obtained by dividing the load by the original area of the cross section of the specimen.

Stress $\sigma = P/Ao$ ( Load/Initial cross-sectional area)

Strain = $e = \Delta l/lo$ (Elongation/Initial gage length)

Engineering stress and strain are independent of the geometry of the specimen.

***Elastic Region:*** The part of the stress-strain curve up to the yielding point. Elastic deformation is recoverable. In the elastic region, stress and strain are related to each other linearly.

Hooke's Law**:** $\sigma = Ee$

The linearity constant E is called the elastic modulus which is specific for each type of material.

***Plastic Region:*** The part of the stress-strain diagram after the yielding point. At the yielding point, the plastic deformation starts. Plastic deformation is permanent. At the maximum point of the stress-strain diagram ***(σUTS),*** necking starts.

***Tensile Strength*** is the maximum stress that the material can support.

$\sigma UTS = Pmax/Ao$

Because the tensile strength is easy to determine and is a quite reproducible property, it is useful for the purposes of specifications and for quality control of a product. Extensive empirical correlations between tensile strength and properties such as hardness and fatigue strength are often quite useful. For brittle materials, the tensile strength is a valid criterion for design.

***Yield Strength*** is the stress level at which plastic deformation starts. The beginning of first plastic deformation is called ***yielding***. It is an important parameter in design. The stress at which plastic deformation or yielding is observed to begin depends on the sensitivity of the strain measurements. With most materials there is a gradual transition from elastic to plastic behavior, and the point at which plastic deformation begins is hard to define with precision. Various criteria for the initiation of yielding are used depending on the sensitivity of the strain measurements and the intended use of the data. ***0,2% off-set method*** is a commonly used method to determine the yield stength. σy(0.2%) is found by drawing a parallel line to the elastic region and the point at which this line intersects with the stress-strain curve is set as the yielding point. An illustration of 0,2% off-set method is shown in the appendix part.

***Ductility*** is the degree of plastic deformation that a material can withstand before fracture. A material that experiences very little or no plastic deformation upon fracture is termed *brittle*.
In general, measurements of ductility are of interest in three ways:
1. To indicate the extent to which a metal can be deformed without fracture in metalworking operations such as rolling and extrusion.
2. To indicate to the designer, in a general way, the ability of the metal to flow plastically before fracture.
3. To serve as an indicator of changes in impurity level or processing conditions. Ductility measurements may be specified to assess material quality even though no direct relationship exists between the ductility measurement and performance in service.

***Resilience*** is the capacity of a material to absorb energy when it is deformed **elastically.**
***Toughness*** is a measure of energy required to cause fracture.
***Poisson's Ratio*** is the lateral contraction per unit breadth divided by the longitudinal extension per unit length.

$$v = -(\Delta d/do)/(\Delta l/lo)$$

### 5.4.1 TESTING SYSTEM

The testing system consists of a tensile testing machine, a load cell, a power supply and an x-y recorder.

***Testing Machine*** is of hydraulic type (Alşa Universal Testing Machine). It is a load-controlled machine.

***Load Cell*** provides an electrical circuit for measuring the instantaneous load along the loading axis.

***Power Supply*** is connected to load cell. It feeds the load cell, amplifies the output signal and displays the load.

***Recorder*** plots the variation of load against time.

### 5.4.2 PROCEDURE

***Before the test***

1. Put gage marks on the specimen
2. Measure the initial gage length and diameter
3. Select a load scale to deform and fracture the specimen. Note that that tensile strength of the material type used has to be known approximately.

***During the test***

1. Record the maximum load
2. Conduct the test until fracture.

***After the test***

1. Measure the final gage length and diameter.
2. The diameter should be measured from the neck.

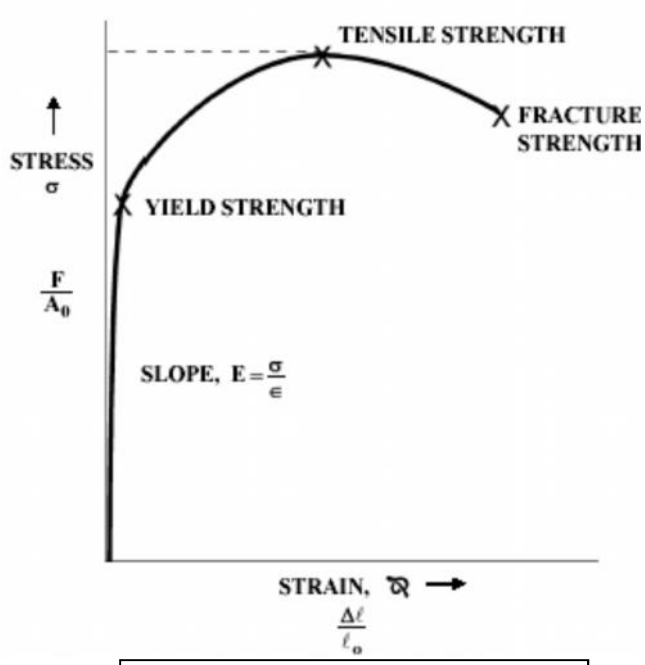


*Figure 5.4: Strain vs Stress Curve*

# Chapter SIX
# Generation of Shock Wave in Shock Tube and Measurement of Time

*Features*

*6.1 Introduction*

*6.2 Mechanism of Shock Wave generation*

*6.3 Shock Tube*

*6.4 Detailed features of shock tube*

*6.5 Shock tube design consideration*

*6.6 Micro-second level time measuring device*

## 6.1 Introduction

The investigation of wave propagation in the free atmosphere is one of the complex experimental works. Experimental investigation is essential to improve the understanding of wave propagation with subsonic or supersonic speed in the free atmosphere. Some optical techniques can able to visualize the propagation and the location of the wave.High speed camera is also used for the

flow visualization to analysis the structure of the wave. The application of some of these techniques to supersonic and hypersonic flows can be highly challenging due to the high velocity, strong gradients and restricted optical access generally encountered. Widely used qualitative and semi-quantitative optical flow diagnostics are shadowgraph, schlieren, and interferometry. Schlieren visualizations of weak shock waves from common phenomena include loud trumpet notes, various impact phenomena that compress a bubble of air, bursting a toy balloon, popping a champagne cork, snapping awooden stick, and snapping a wet towel. The balloon burst, snapping a ruler on a table, and snapping the towel and a leather belt all produced readily visible shock wave phenomena. Doig et al 2008 conducted experiment where directionindicating color schlieren flow visualization was used to determine optically the general effectiveness of the methods. Multiple images were taken during a single tunnel run, which allowed, to some extent, confirmation of the general steadiness of the flow. The light source used in the experiments had a flash duration of 200 μs , which was short enough to 'freeze' any large-scale motions in the flow but long enough to average out small-scale fluctuations such as free-stream turbulence and boundary layer effects on the test section windows.

Laser-based techniques such as laser Doppler anemometry and particle image velocimetry are well established for investigation of supersonic flows, but as yet their use in hypersonic flows has been limited. Other relevant measurement techniques include particle tracking velocimetry, Doppler global velocimetry, laser-two-focus anemometry, background oriented schlieren and laser induced fluorescence methods, molecular tagging velocimetry for velocity measurement and thermo-graphic phosphor thermometry for surface temperature measurement. Laser measurement techniques are becoming more commonly applied to many areas of thermo-fluids and heat transfer. An area of their application, which presents highly challenging requirements, is in the measurement of aerospace flows. In the shock wave research laboratory, Tohoku University Japan, the speed of projectile was measured by Shimadzu's HPV-1 High Speed Video Camera and the time elapsed from recording the first frame up to the 100th frame was only about one ten-thousandth of a second. The ability to record dynamic images over short intervals is extremely significant. In the other technique, the projectile location can be determined by locating the trajectory of an incoming projectile. All supersonic projectiles are accompanied by a bow wave, often referred to as the "Mach Cone" which is virtually attached to the ogive of the

projectile and which can be detected acoustically. When a distributed array of microphones detect the arrival of this cone, it is possible to calculate the position and angle of the trajectory from the microphone data. In the study of metal-high explosive detonation wave interaction, by the pin technique, it is desirable to obtain time measurements to an accuracy of less than 1 mμsec over a total time interval of 5 μsec. Commercial instruments capable of a high degree of time resolution were not available and a special instrument was developed for this purpose. A cathode-ray oscilloscope, displaying deflection type event pulses, is converted into a precise time-measuring instrument by a calibrated zig-zag sweep. The record is obtained by single-shot photography of the cathode-ray tube sweep which is triggered by the event to be measured. Kobiera et al 2009 conducted experiment on the shock wave propagation through the test section and the shock wave causes a disturbance of the droplets; this process was visualized by a schlieren system and recorded by a high-speed camera. The camera was synchronized with the igniter that was connected to the spark plug mounted in the driver section. The test section was also equipped with a pressure measurement system (two pressure sensors and amplifiers) whose signals are recorded on an oscilloscope. The sensors were located ahead of the test section windows, and can be used to measure the shock velocity and pressure waveform. Pianthong et al 2002 conducted experiment with the use of the shadowgraph method, showing the projectile traveling inside and leaving the pressure relief section at a velocity of about 1100 m/s. they also visualized the supersonic diesel fuel jets (velocity about 2 km/s ) by the shadowgraph method.

In the present method, metal to metal touch switches generate pulses for triggering which open and close the gate to allow and stop the crystal frequency for counting. Using the number of pulse counted, the traveling time between the trigger points is measured for the subsonic or supersonic objects. Due to pressure difference across the wave, the trigger is operated by the pressure response to detect the wave position in the open atmosphere. This is one of the easier methods to measure the traveling time of the subsonic or supersonic wave between the two trigger points as compare to other methods. Even visualizations of the wave front or the pressure response from pressure transducers are the familiar methods to measure the strength of the wave or its locations but the present technique is more reliable and accurate to measure the time. Normally the propagation time of the logic gates is not more than 20 nanoseconds, so the accuracy level of the measured time will be less than 0.006%.

## 6.2 Mechanism of shock wave generation

An air compressor is connected with the pressure chamber first. The wiper of the pressure gauge set on the pressure chamber starts deflecting. The principle condition of the shock wave generation is fulfilled as the chamber pressure rises up to 5 to 6 atmosphere.

Then by the help of manfully operated penetrator plastic diaphragm attached in the junction of the pressure chamber and the following section, the intermittent section tube is then blown up. The shock wave is then generated and propagated. The direction of the shock wave and the expansion wave is exactly opposite.

## 6.3 Shock Tube

A shock tube is a device used primarily to study the generation and propagation of shock wave under a given set of conditions. It's also used for gas phase combustion reactions. Shock tubes (and related impulse facilities: shock tunnels, expansion tubes and expansion tunnels) can also be used to study aerodynamic flow under wide range of temperatures and pressures that are difficult to obtain in other types of testing facilities.

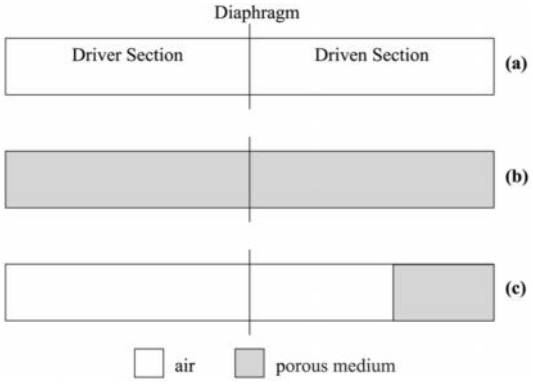


*Figure 6.1: A Shock Tube showing different sections*

Considering the mechanism that the shock wave follows during propagation the shock tube can be assembled to have two main sections.

1. Driver Section
2. Driven Section

**Driver section**: The pressure chamber in which the pressure is initially been heaped up is known as the driver section. It causes the shock front to propagate through the downstream.

**Driven section**: The section following the driver section is known as the driven section. It may consist of several sections like intermittent section; square section etc. pressure inside the driven section is less than the driven section.

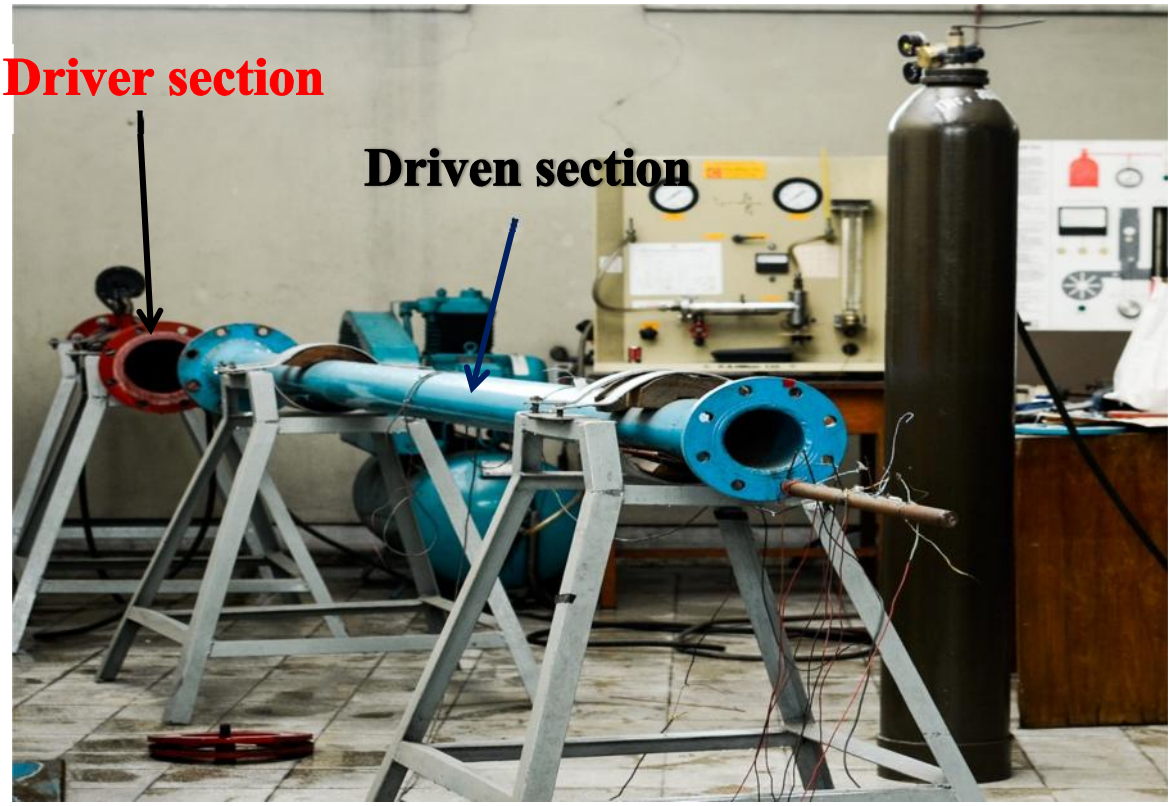


***Figure 6.2: Shock Tube used in our experiment***

## 6.3.1 Application of the shock tube

- Shock tubes have numerous applications in combustion and aerodynamics studies.
- For aerodynamic testing the fluid flows induced in the driven section behind the shock wave can be used as much as wind tunnel is used.
- Shock tubes allow the study of fluid flow at temperatures pressures that would difficult to obtain in wind tunnels.
- A further development for aerodynamic testing in the shock tunnel where a nozzle is placed between the end of the tube and a dump tank.

## 6.4 Detailed Features of the Shock Tube Used

| | |
|---|---|
| **Type** | Horizontal |
| **Wave Propagation direction** | Towards open atmosphere |
| **Shock tube Segments** | Pressure chamber<br>Intermittent tube<br>Square sectional tube |

*Table 8.1 Key Features of Shock Tube Used*

| **Element** | **Material** |
|---|---|
| Pressure chamber(Dia 5 inch) | Mild steel |
| Intermittent duct(dia 4 inch) | Mild steel |
| Square sectioned tube(10*10 inch) | Mild steel |
| Flange | Mild steel |
| Fastener Steel | Steel |
| Diaphragm | Different types of Celluloid |
| Gasket | Rubber |
| Threaded nipple | Mild steel |
| Penetrator | Mild steel |

## 6.5 Shock tube design consideration

Pressure chamber and the intermittent tube: Since the generation of the shock tube is associated with the sudden increase of temperature, pressure, density etc of the surrounding, the shock tube material should be such that it can withstand the required conditions of shock wave generation,

In our case, we have used mild steel for making shock tube for the following reasons:

- Improved strength at ordinary temperatures.
- Improved mechanical properties at higher temperatures
- Improved hardness at any minimum hardness or strength

**6.5.1 Gasket:** The experiments deal with high pressure air. This compressed air has got pressure well above the atmospheric one (minimum 5 to 6 atmosphere).For the balance in pressure with the atmosphere the compressed air tends to leak from the chamber which is not desirable at all. To prevent this leakage, rubber gaskets are used between flanges at the ends of the pressure chamber.

**6.5.2 Diaphragm:** A diaphragm, also known as a bursting disc or rupture disc, is a non-reclosing pressure relief device that, in most uses, protects a pressure vessel, equipment or system from over pressurization or potentially damaging vacuum conditions. A rupture disc is a type of sacrificial part because it has a one-time-use membrane that fails at a predetermined differential pressure, either positive or vacuum.

The diaphragm material should be such that that it is flexible plastic and not brittle. Brittle diaphragm are mostly susceptible to early failure which will not eventually fulfill the objective of the experiment, These properties allow the diaphragm to withstand pressure at the experimental condition leading to towards a desirable and correct result.

## 6.6 Micro-second level time measuring device

Generally pressure transducer and oscillator are used to measure the velocity of the shock wave. In our experiment we have developed and used a special device for measuring the speed of the shock wave. It measures the number of pulses generated by crystal resonator as the wave travels between two triggers. The layout of the device shown below:

*Components of the supersonic speed measuring device*

- Quartz crystal having a frequency of *3.579540 MHz*.
- Motorola *MC141518B* Dual counter

- Motorola MC141518B BCD-to-seven segment latch.
- Bread board.
- Logic gate
- 7-segment display.
- Triggers made of metal wires.
- Battery.


*Figure 6.3: Micro-second level time measuring device*

## 6.6.1 Principle of micro-second level time measuring device

In the device quartz crystal having a frequency of 3.579540 MHz is used as the crystal resonator. The crystal resonator is connected to the logic gate through which pulse signal goes to the counter. Two triggers are used to close and open the gate. Metal to metal contact is used for triggering. The triggers use the interlocking system to ensure the accuracy of the operation as there is high possibility of consecutive touches between the metals after the first touch. Once the metal wire touches the metal wire loop and displaced thereby it will send signal to the gate to open or close. First trigger open the gate and second trigger closes the gate. By counting the pulses counter gives signal to the seven segments display.7 segment display shows the number of pulses generated by the crystal during the time interval of two contacts. By calculation, time taken by the wave to travel between two triggers can be measured from the display.

If takes t seconds for the wave to travel between two triggers and N no. of pulses were generated then the time t can be calculated as follows.

3579540 pulses are generated in 1 second

N pulses will be generated in (1/3579540) *N seconds.

If s is the distance between two triggers in the direction of flow then the speed of flow can be calculated using the formula,

$$\text{Velocity of flow} = \frac{\text{Distance between the triggers}}{\text{Time needed for the wave travel between the triggers}} = \frac{s}{t}$$

## 6.6.2 Crystal Resonator

The quartz crystal is a piezoelectric substance. A piezoelectric substance is one that produces an electric charge when a mechanical stress is applied (the substance is squeezed or stretched). Conversely, a mechanical deformation (the substance shrinks or expands) is produced when an electric field is applied. This effect is formed in crystals that have no center of symmetry. To explain this, we have to look at the individual molecules that make up that crystal.

Each molecule has a polarization, one end is more negatively charged and the other end is positively charged, and is called a dipole. This is a result of the atoms that make up the molecule and the way the molecules are shaped. The polar axis is an imaginary line that runs through the center of both charges on the molecule. In a mono crystal the polar axis of all of the dipoles lie in one direction. The crystal is said to be symmetrical because if you were to cut the crystal at any point, the resultant polar axes of the two pieces would lie in the same direction as the original. In a polycrystal, there are different regions within the material that have a different polar axis.

*Figure 6.4: Crystal Used in our experiment*

It is asymmetrical because there is no point at which the crystal could be cut that would leave the two remaining pieces with the same resultant polar axis.

The quartz crystal (like any elastic material) has a precisely defined natural frequency (caused by its shape and size) at which it prefers to oscillate, and this is used to stabilize the frequency of a periodic voltage applied to the crystal.

The piezoelectric crystal bends in different ways at different frequencies. This bending is called the vibration mode. The crystal can be made into various shapes to achieve different vibration modes. To realize small, cost effective, and high performance products, several modes have been developed to operate over several frequency ranges. These modes allow us to make products working in the low kHz ranges up to the MHz range.

An important group of piezoelectric materials are ceramics. Murata utilizes these various vibration modes and ceramics to make many useful products, such as ceramic resonator, Ceramic band pass filter, ceramic discriminator, ceramic traps, SAW filters and buzzers.

### 6.6.3 Counter

A counter is a device which stores (and sometimes displays) the number of times a particular event or process has occurred, often in relationship to a clock signal. In practice, there are two types of counters:

- Up counters, which increase (increment) in value
- Down counters, which decrease (decrement) in value

In electronics, counters can be implemented quite easily using register-type circuits such as the flip-flop, and a wide variety of designs exist, e.g.:

- Asynchronous (ripple) counter – changing state bits are used as clocks to subsequent state flip-flops
- Synchronous counter – all state bits change under control of a single clock
- Decade counter – counts through ten states per stage
- Up–down counter – counts both up and down, under command of a control input
- Ring counter – formed by a shift register with feedback connection in a ring
- Johnson counter – a twisted ring counter
- Cascaded counter

Each is useful for different applications. Usually, counter circuits are digital in nature, and count in natural binary. Many types of counter circuit are available as digital building blocks, for example a number of chips in the 4000 series implement different counters.

Occasionally there are advantages to using a counting sequence other than the natural binary sequence—such as the binary coded decimal counter, a linear feedback shift register counter, or a Gray-code counter. Counters are useful for digital clocks and timers, ers are useful for digital clocks and timers, and in oven timers, VCR clocks, etc.

## 6.6.4 MC14518B .5 dual BCD Counter

The MC14518B dual BCD counter and the MC14520B dual binary counter are constructed with MOS P-channel and N-channel enhancement mode devices in a single monolithic structure. Each consists of two identical, independent, internally synchronous 4-stage counters. The counter stages are type D flip-flops, with interchangeable Clock and Enable lines for incrementing on either the positive-going or negative-going transition as required when cascading multiple stages. Each counter can be cleared by applying a high level on the Reset line. In addition, the MC14518B will count out of all undefined states within two clock periods. These complementary MOS up counters find primary use in multi-stage synchronous or ripple counting applications requiring low power dissipation and/or high noise immunity.

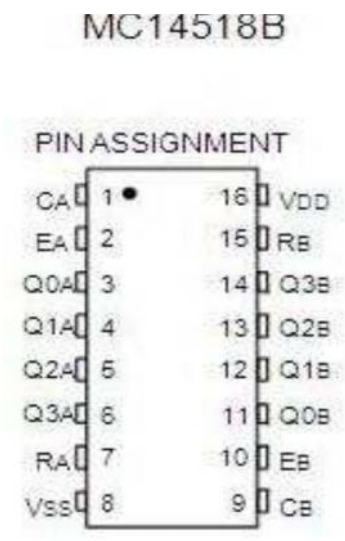


*Figure 6.5: Pin assignment of Motorola MC14518B dual*

***Features***

- Diode Protection on All Inputs
- Supply Voltage Range = 3.0 Vdc to 18 Vdc
- Internally Synchronous for High Internal and External Speeds.
- Logic Edge- Clocked Design Increment on Positive Transition of Clock or Negative Transition on Enable
- Capable of Driving Two Low-power TTL Loads or One Low-power Schottky TTL. Load Over the Rated Temperature Range

## 6.6.5 7-segment display

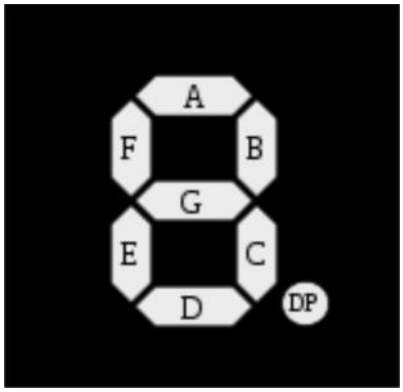


*Figure 6.6: 7-segments*

A seven-segment display, or seven-segment indicator, is a form of electronic display device for displaying decimal numerals that is an alternative to the more complex dot-matrix displays. Seven-segment displays are widely used in digital clocks, electronic meters, and other electronic devices for displaying numerical information.

A seven segment display, as its name indicates, is composed of seven elements. Individually on or off, they can be combined to produce simplified representations of the Arabic numerals. Often the seven segments are arranged in an oblique (slanted) arrangement, which aids readability. In most applications, the seven segments are of nearly uniform shape and size (usually elongated hexagons, though trapezoids and rectangles can also be used), though in the case of adding machines, the vertical segments are longer and more oddly shaped at the ends in an effort to further enhance readability.

Each of the numbers 0, 6, 7 and 9 may be represented by two or more different glyphs on seven-segment displays

The seven segments are arranged as a rectangle of two vertical segments on each side with one horizontal segment on the top, middle, and bottom. Additionally, the seventh segment bisects the rectangle horizontally. There are also fourteen-segment displays and sixteen-segment displays (for full alphanumeric); however, these have mostly been replaced by dot-matrix displays.

The segments of a 7-segment display are referred to by the letters A to G, as shown to the right, where the optional DP decimal point (an "eighth segment") is used for the display.

## 7-Segment Numeric LED Displays

In industrial PLC applications, one of the old, but simpler methods of displaying numeric information is to use one or more 7-Segment numeric displays connected to an output card of a

PLC... Although it is possible to build such a display yourself, it is far more common to employ a pre-manufactured product such as the 4-digit panel mount unit shown at the top of this page...

To correctly interface a PLC to such a display, it helps to first understand what basic electronic components are typically employed in their makeup, and how this effects our task of interfacing to, and programming such a unit... Although both LED and LCD numeric displays are readily available, and interfaced similarly, we'll concentrate on the more common LED units in the examples to follow...

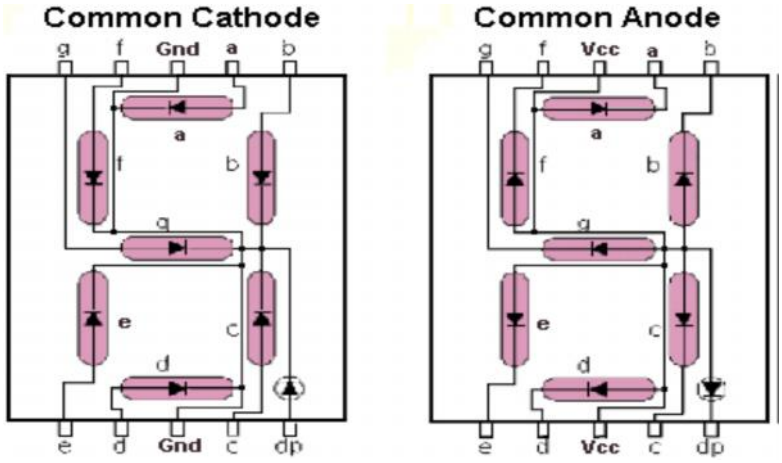


## 6.6.6 MC14518B BCD-to-seven segment latch

The MC14511B BCD-to-seven segment latch/decoder/driver is constructed with complementary MOS (CMOS) enhancement mode devices and NPN bipolar output drivers in a single monolithic structure. The circuit provides the functions of a 4-bit storage latch, an 8421 BCD-to-seven segment decoder, and an output drive capability. Lamp test (LTbar), blanking (BIbar), and latch enable (LE) inputs are used to test the Display to turn-off or pulse modulate the brightness of the Display and to store a BCD code, respectively. It CAN be used with seven-segment light-emitting Diodes (LED), incandescent, fluorescent, gas discharge, or liquid crystal readouts either directly or indirectly. Applications include instrument (e.g., Counter DVM, etc.) Display driver, computer/calculator Display driver, cockpit Display driver, and various Clock watch, and Timer uses.

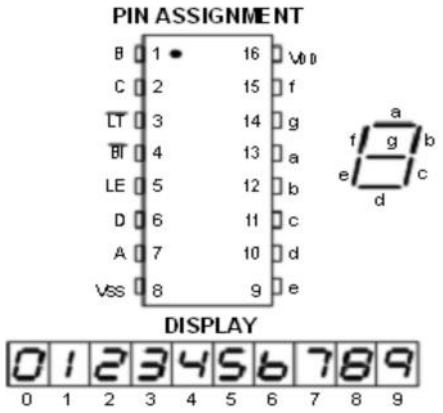


*Figure 6.7: Pin assignment of MC14511B BCD to seven segment latch*

TRUTH TABLE

| Inputs | | | | | | | Outputs | | | | | | | |
|---|---|---|---|---|---|---|---|---|---|---|---|---|---|---|
| LE | $\overline{BI}$ | $\overline{LT}$ | D | C | B | A | a | b | c | d | e | f | g | Display |
| X | X | 0 | X | X | X | X | 1 | 1 | 1 | 1 | 1 | 1 | 1 | 8 |
| X | 0 | 1 | X | X | X | X | 0 | 0 | 0 | 0 | 0 | 0 | 0 | Blank |
| 0 | 1 | 1 | 0 | 0 | 0 | 0 | 1 | 1 | 1 | 1 | 1 | 1 | 0 | 0 |
| 0 | 1 | 1 | 0 | 0 | 0 | 1 | 0 | 1 | 1 | 0 | 0 | 0 | 0 | 1 |
| 0 | 1 | 1 | 0 | 0 | 1 | 0 | 1 | 1 | 0 | 1 | 1 | 0 | 1 | 2 |
| 0 | 1 | 1 | 0 | 0 | 1 | 1 | 1 | 1 | 1 | 1 | 0 | 0 | 1 | 3 |
| 0 | 1 | 1 | 0 | 1 | 0 | 0 | 0 | 1 | 1 | 0 | 0 | 1 | 1 | 4 |
| 0 | 1 | 1 | 0 | 1 | 0 | 1 | 1 | 0 | 1 | 1 | 0 | 1 | 1 | 5 |
| 0 | 1 | 1 | 0 | 1 | 1 | 0 | 0 | 0 | 1 | 1 | 1 | 1 | 1 | 6 |
| 0 | 1 | 1 | 0 | 1 | 1 | 1 | 1 | 1 | 1 | 0 | 0 | 0 | 0 | 7 |
| 0 | 1 | 1 | 1 | 0 | 0 | 0 | 1 | 1 | 1 | 1 | 1 | 1 | 1 | 8 |
| 0 | 1 | 1 | 1 | 0 | 0 | 1 | 1 | 1 | 1 | 0 | 0 | 1 | 1 | 9 |
| 0 | 1 | 1 | 1 | 0 | 1 | 0 | 0 | 0 | 0 | 0 | 0 | 0 | 0 | Blank |
| 0 | 1 | 1 | 1 | 0 | 1 | 1 | 0 | 0 | 0 | 0 | 0 | 0 | 0 | Blank |
| 0 | 1 | 1 | 1 | 1 | 0 | 0 | 0 | 0 | 0 | 0 | 0 | 0 | 0 | Blank |
| 0 | 1 | 1 | 1 | 1 | 0 | 1 | 0 | 0 | 0 | 0 | 0 | 0 | 0 | Blank |
| 0 | 1 | 1 | 1 | 1 | 1 | 0 | 0 | 0 | 0 | 0 | 0 | 0 | 0 | Blank |
| 0 | 1 | 1 | 1 | 1 | 1 | 1 | 0 | 0 | 0 | 0 | 0 | 0 | 0 | Blank |
| 1 | 1 | 1 | X | X | X | X | | | | * | | | | * |

X = Don't Care
*Depends upon the BCD code previously applied when LE = 0

*Figure 6.8: Truth table for MC14511B BCD to seven segment latch*

# Chapter SEVEN
# Determination of Diaphragm Rupturing Phenomena

***Features***

***7.1 Introduction***

***7.2 Diaphragm Material Selection***

***7.3 Measurement of Tensile Strength***

***7.4 Measurement of Hardness***

***7.5 Shock Tube Test***

***7.6 Rupturing Condition of the Diaphragms***

## 7.1 Introduction

Shock Wave generation in shock tube now a days very important for Shock Wave study in different fields. For educational purpose the student must visualize what is Shock Wave and it's properties but it is not possible for them to study shock wave outside every time so shock tube is used to study shock tube. On the other hand shock wave is so important for different Chemical

study so in laboratory they need shock wave which is only possible by shock tube. In Pharmaceutical evaluation Shock Wave is used very frequently. In medical field Shock Wave becoming very important, in different treatment shock wave is used which was not possible without shock wave. Such as Extracorporeal shock wave lithotripsy (ESWL) is a non-invasive treatment of kidney stones (urinary calculosis) and biliary calculi (stones in the gallbladder or in the liver) using an acoustic pulse. There are also many applications.

In metallurgy shock wave also used i.e. Shock hardening is a process used to strengthen metals and alloys, wherein a shock wave produces atomic-scale defects in the material's crystalline structure. As in cold work, these defects interfere with the normal processes by which metallic materials yield (plasticity), making materials stiffer, but more brittle. When compared to traditional cold work, such an extremely rapid process results in a different class of defect, producing a much harder material for a given change in shape. If the shock wave applies too great a force for too long, however, the rarefaction front that follows it can form voids in the material due to hydrostatic tension, weakening the material and often causing it to spall. Since voids nucleate at large defects, such as oxide inclusions and grain boundaries, high-purity samples with a large grain size (especially single crystals) are able to withstand greater shock without spalling, and can therefore be made much harder.

So for creating Shock Wave in shock we must produce supersonic flow in the shock tube. For this the pressure at the driven section must be high enough to create a supper sonic air flow. Without high pressure larger Mach Number is not possible which is more desirable in shock wave formation. In Shock Tube the Diaphragm is the main element which takes the pressure during shock wave creation. So Diaphragm should be much stronger to withstand this much pressure in the driven section of the shock tube. If the Diaphragm dose not capable of holding much pressure which is needed to create shock then the shock tube experiment will be in vain. So for the proper shock wave creation we must select the Diaphragm suitably and also economically.

### 7.1.1 Diaphragm

A Diaphragm, also known as a bursting disc or rupture disc, is a non-reclosing pressure relief device that, in most uses, protects a pressure vessel, equipment or system from over pressurization or potentially damaging vacuum conditions. A rupture disc is a type of sacrificial part because it has a one-time-use membrane that fails at a predetermined differential pressure, either positive or vacuum.

## 7.2 Diaphragm Material Selection

As we discussed Diaphragm is very important for the shock wave generation in shock tube so the selection of Diaphragm material is very important issue. The Diaphragm material should be Hard and Tough to withstand high amount of pressure to generate supersonic flow for large Mach number. Also the material must be cheap and available in the market for random use.
We here selected Celluloid as Diaphragm. In market different types of celluloid are availableAt cheap price. We took three kinds of celluloid for our experiment.

**Materials for the Diaphragm:**

1. **X-ray film**
2. **Rexine (Called in Market)**
3. **Celluloid Sheet**

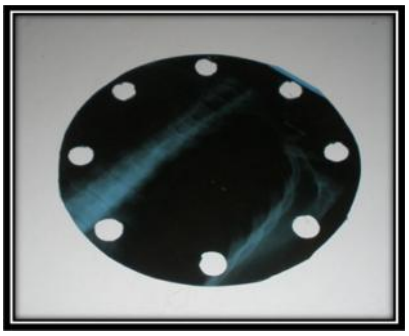

***Figure 7.1: X-ray film***

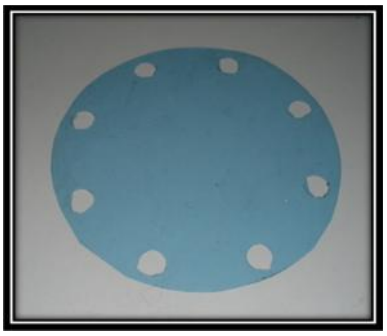

***Figure 7.2: Rexine***

***Figure 7.1: Celluloid Sheet***

## 7.3 Measurement of Tensile Strength

For the measurement of tensile strength we took three stripes of the three materials.

**Size of the Stripes :**

- **Length: 250 mm**
- **Width: 45 mm**

**X-RAY FILM STRIPE**

**REXINE STRIPE**

**CELLULOID SHEET STRIPE**

***Figure7.4: Celluloid Stripes***

## 7.3.1 Tensile Strength in UNIVERSAL MATERIAL TESTING MACHINE:

Then we went to the **UNIVERSAL MATERIAL TESTING MACHINE** to measurer the tensile strength of the materials. The Stripes are clamped in the UNIVERSAL MATERIAL TESTING MACHINE tightly then applied load to the materials. With the increase of load there was certain displacement on the Stripes. With the increase of the load there displacement increases. After applying a certain amount of load the Stripes do not take any load and by the increase of displacement the load decreases. The highest load is taken is the Ultimate Tensile Strength of the material. We tabulated the load and displacement and then plotted in graph.

***Figure7.5: Universal Material Testing Machine***

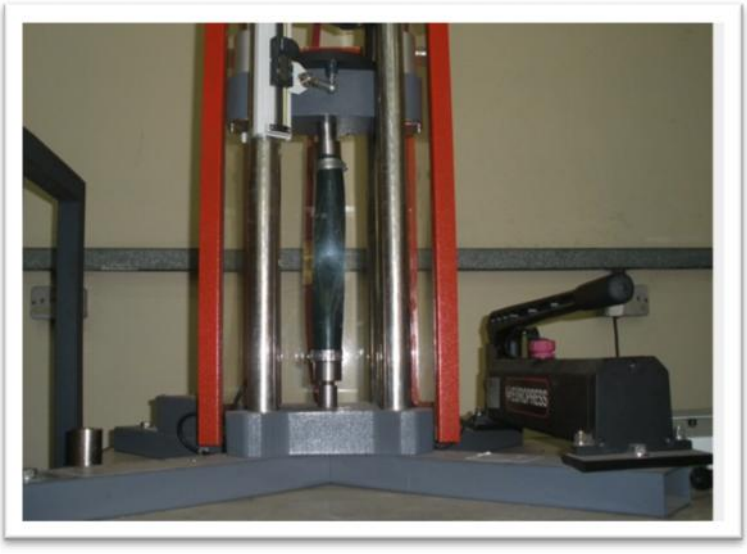

***Figure 7.6: Measurement of Tensile Strength in Universal Material Testing Machine***

### 7.3.2 Ultimate Tensile Strength of X-ray Film

After testing the ultimate tensile strength of the X-ray film we have experienced that the X-ray film has ultimate tensile strength about 0.8 kN. First with increase of load the displacement of the X-ray stripe increases and with the more loads it continues. When the load becomes 0.8 kN with the pressing of the load applying lever the stripe do not take any further load but the displacement continues. That was the ultimate tensile strength of the X-ray film, and after that plastic deformation starts. After that the stripes begins to free the load and with the pressing load applying lever it displaced but load dose not increases. And applying more load after a certain period the stripe torn out.

The Force vs Displacement curve of the X-ray film is given bellow which will give us idea about the ultimate tensile strength.

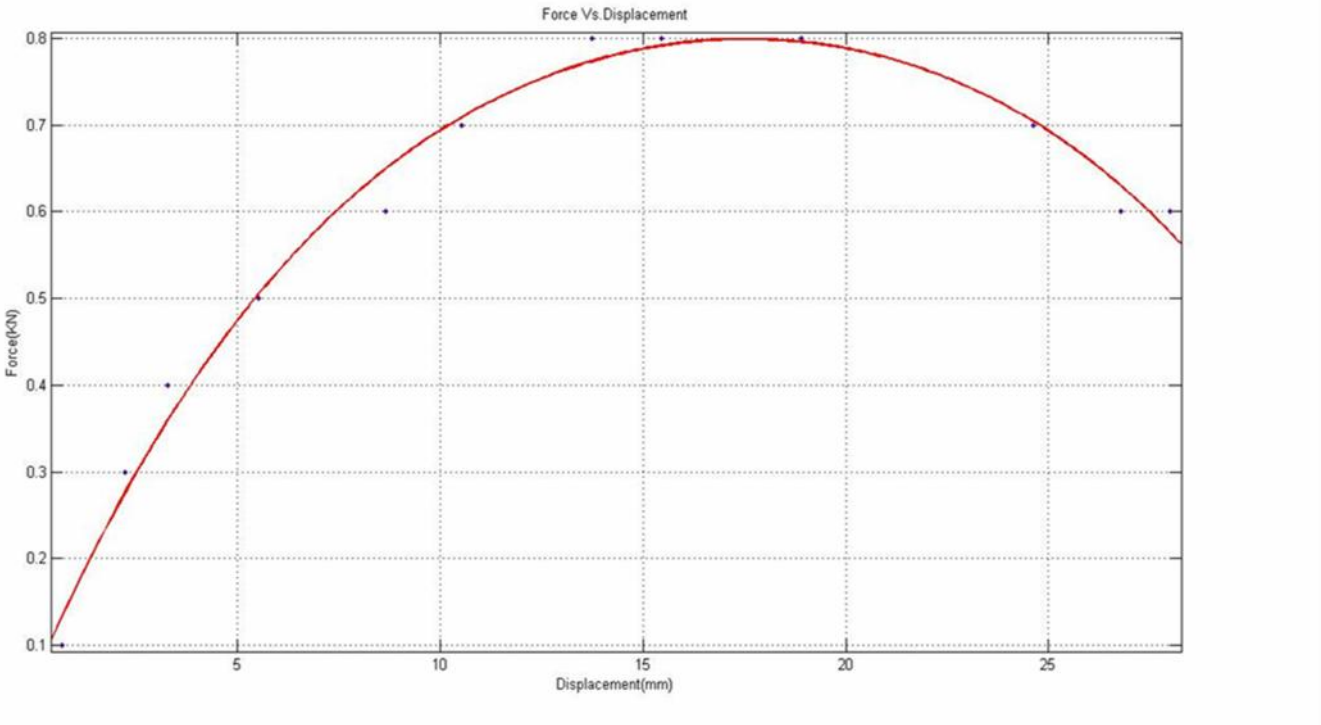


***Figure 7.7: Force vs Displacement curve of the X-ray film***

### 7.3.3 Ultimate Tensile Strength of Rexine

After testing the ultimate tensile strength of the Rexine we have experienced that the X-ray film has ultimate tensile strength about 0.7 kN. First with increase of load the displacement of the Rexine stripe increases and with the more loads it continues. When the load becomes 0.7 kN with the pressing of the load applying lever the stripe do not take any further load but the displacement continues. That was the ultimate tensile strength of the Rexine, and after that plastic deformation starts. After that the stripes begins to free the load and with the pressing load applying lever it displaced but load dose not increases. And applying more load after a certain period the stripe torn out.

The Force vs Displacement curve of the Rexine is given bellow which will give us idea about the ultimate tensile strength.

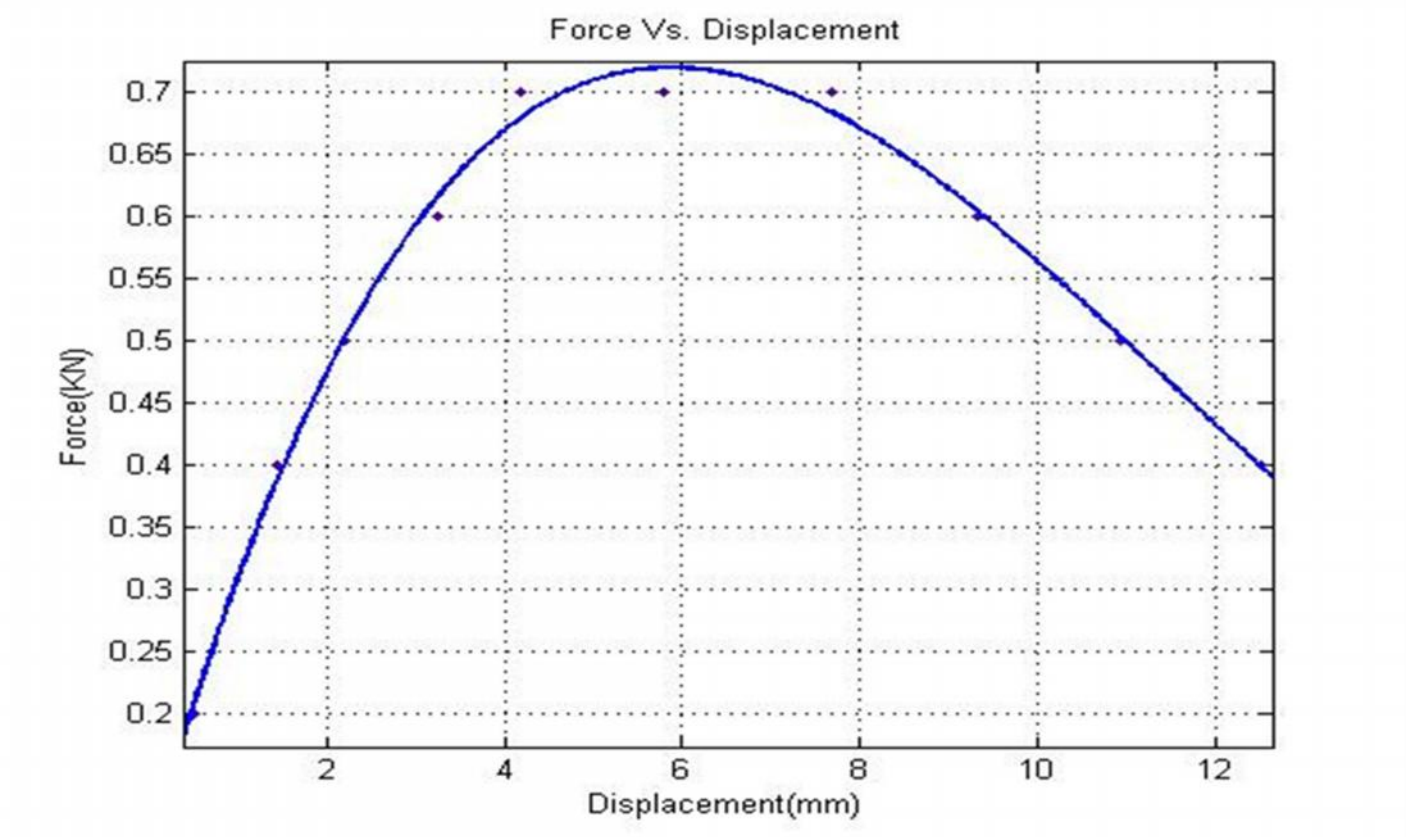


***Figure 7.8: Force vs Displacement curve of the Rexine***

### 7.3.4 Ultimate Tensile Strength of Celluloid Sheet

For the plastic Celluloid Sheet the ultimate tensile strength was unsatisfactory. When we applied force to the lever at the beginning the stripe did not take any load, but there was displacement of. With the increase of the pressure in the lever the displacement increases and after a certain deformation it took 0.1 kN load. And with further displacement the stripe did not take more loads, it was constant about 0.1 kN for a long period time. And the deformation continues with the increase of pressure on the lever.

The Force vs Displacement curve of the Celluloid Sheet is given bellow which will give us idea about the ultimate tensile strength.

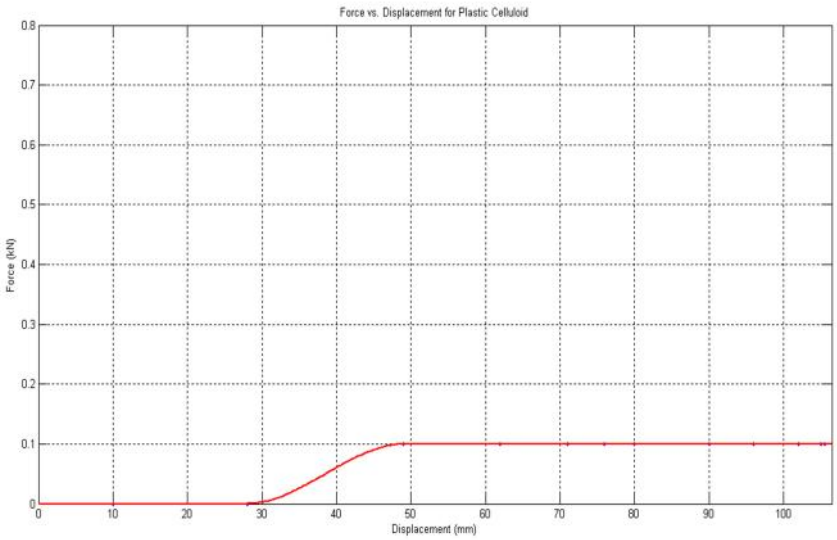


***Figure 7.9: Force vs Displacement curve of the Celluloid Sheet***

## 7.4 Measurement of Hardness

For the measurement of Hardness we used Rockwell Hardness Testing Machine. We took the materials to the hardness tester and measure the Hardness. We performed the hardness test on different positions. Thus we calculated the average value for each material.

*Figure 7.10: Measurement of Hardness Rockwell Hardness Testing Machine*

**Indenter: 1⁄16-inch-diameter (1.588 mm) Steel Sphere.**

**Load: 60 kg**

**Scale: B Scale**

### 7.4.1 Hardness of three materials:

| X-ray Film | | Rexine | | Celluloid Sheet | |
|---|---|---|---|---|---|
| **Hardness (B Scale)** | **Average** | **Hardness (B Scale)** | **Average** | **Hardness (B Scale)** | **Average** |
| 70 | | 74 | | 37 | |
| 70 | | 75 | | 35 | |
| 71 | 70 | 74 | 74 | 37 | 37 |
| 70 | | 74 | | 38 | |
| 69 | | 74 | | 39 | |

## 7.5 Shock Tube Test

### 7.5.1 Experimental Setup

The time measuring device has been constructed to measure the subsonic or supersonic wave propagation time in microsecond level in the free atmosphere. A piezoelectric crystal type HOSONIC, D349 which generates 3579540 pulses per second is used to measure the traveling time in micro-second level for any subsonic or supersonic objects in free atmosphere.

Metal to metal touch switches generate pulses for triggering which open and close the gate to allow and stop the crystal frequency for counting. A direct metal to metal contact triggering is more efficient as compare to other sensing devices, like pressure transducers, Electro-optic sensors, Infrared sensors, Magnetic sensors etc.

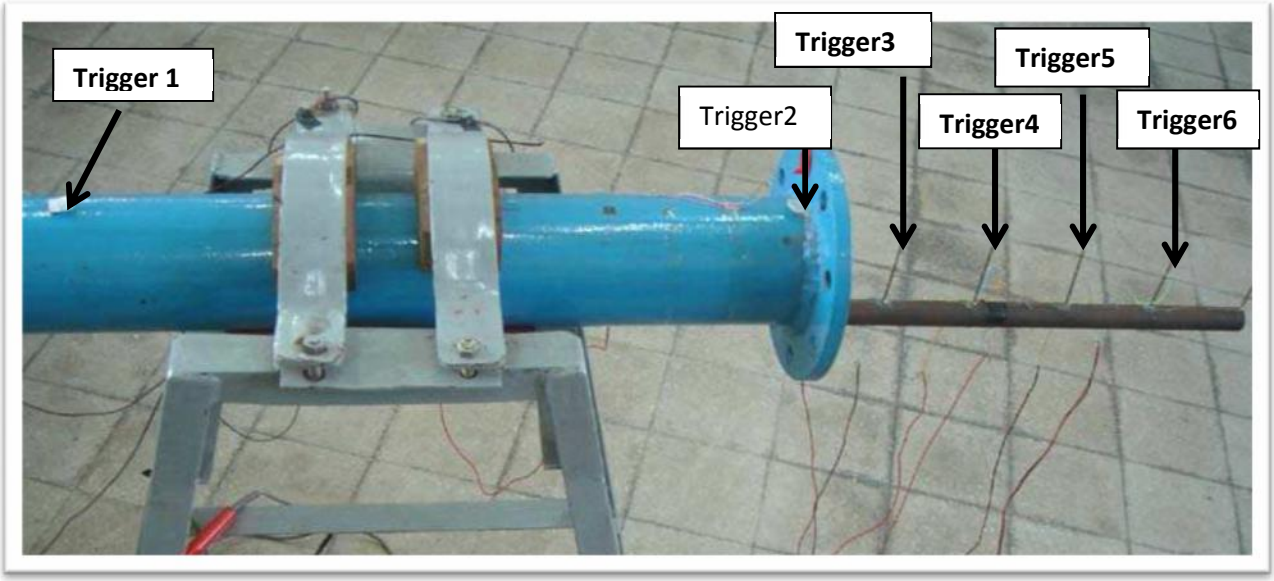


***Figure 7.11: Shock tube and the position of Triggers***

Using the number of pulse counted, the traveling time difference between the trigger points is measured for the subsonic or supersonic objects. To conduct an experiment on subsonic or supersonic objects, a shock tube is constructed in the Fluid Mechanics Laboratory of IUT for

wave propagation in the free atmosphere. A compressor of 10kg/cm2 pressure range is used to raise the air pressure in the pressure chamber of the shock tube. The diameter and length of the pressure chamber is 15 cm and 1.5 m. The dimensions of the driven section of the shock tube are 10 cm diameter and 5 m long. Due to sudden rupture of the diaphragm for the chamber pressure of range 3.5 – 4.5 kg/cm2; a wave generates in a shock tube which travels with subsonic speed. If pressure range increases, a supersonic shock wave generates. Two trigger points (Trigger-1 and Trigger-2) are installed 61.5 cm apart in the shock tube to measure the incident wave Mach number. Similarly other 2-5 trigger points are also installed at different positions by the support, shown in Fig.7.4, in the free space to measure the wave speed during the propagation in the free atmosphere and the measured traveling times between different triggers are recorded.

### 7.5.2 Procedure of the project execution

- The fastener (i.e. nuts and bolts) adjoining the sections, pressure chamber and the intermittent section is undone.
- The diaphragm cut in the shape of the cross section of the conjunction of the sections is thus placed along with the gasket.
- The sections are again adjoined together by the help of fasteners.

***Figure 7.12: Fitting of Diaphragm in the Shock Tube***

- The travelling time for the first two triggers the for incident shock wave was measured by the single channeled microsecond level time measuring device
- For trigger 3 and 4 which were placed just after the shock tube in the open atmosphere the travelling time was measured with the help of oscilloscope.
- From trigger 4 to trigger 6 the travelling time was measured by the double channeled microsecond level time measuring device.
- In our experiment the outlet of the compressor was turned off.
- Air compressor was turned on.
- The outlet hose of the compressor is then connected to the inlet of the pressure chamber.
- The outlet valve of the air compressor is gradually turned on.
- The inlet valve of the pressure chamber was gradually turned on
- The pressure in the chamber started to rise up.
- The diaphragm between the tube sections must be strong enough to hold the initial pressure difference but also must burst cleanly to yield good test results.
- High pressure was obtained inside the chamber and the inlet valve was then closed.
- The distended diaphragm was clearly visible in the bare eyes.

***Figure 7.13: Diaphragm condition after Shock generation***

- The diaphragm was then blown up with the help of diaphragm penetrator apparatus.
- After the diaphragm was burst a compression wave travelled down the tube into the driven section, which then rapidly steepened to form a shock front known as the incident shock wave.
- This shock wave increased the pressure and the temperature of the driven gas and induced a flow in the direction of the shock wave.
- Simultaneously a rarefaction wave often referred to as an expansion wave travelled back into the driver gas.
- The circular section that represents the interface separating the driven gas and the driver gas is called the contact surface.
- The contact surface moved rapidly along the tube behind the shock tube.
- The triggers of the instruments are kept in a certain distance.

***Figure 7.14: Shock Wave generated in our Experiment***

### 7.5.3 Incident Shock Wave (Inside the Shock Tube):

Chamber pressure=4.2kg/square cm

Distance between the trigger points for

Incident wave= 61.5cm.

Travelling time in the shock tube = 2200 μsec

Velocity of the wave = $\frac{61.5\times10^{-2}}{2200\times10^{-6}}$ $ms^{-1}$

=279.55 $ms^{-1}$


Sound velocity= $\sqrt{kRT}$

= $\sqrt{1.4 \times 287 \times 307}$ $ms^{-1}$

= 351.2 $ms^{-1}$

Incident Mach number =$\frac{279.551}{351.2}$

= 0.8


***Figure 7.15: Experimental result obtained in (a) Single- Channeled; (b) Double Channeled micro-second level time measuring***

## 7.6 Rupturing Condition of the Diaphragms

After generating shock wave in shock tube the Diaphragm is ruptured. As we used three kind of Celluloid as our Diaphragm, so the rupturing of the diaphragms are not same. Different types of diaphragm ruptured differently. The Diaphragm rupturing characteristics for different types of Diaphragms are given below.

**7.6.1 X-RAY FILM:** It took more pressure around 4.5 kg/cm$^2$ and gave better MACH number about "M=1.2". And diaphragm ruptured into different parts. And this Diaphragm shows more suitable properties to generate shock in shock tubes. The Diaphragm ruptured uniformly. The rupturing condition of the X-ray film is shown in the figure

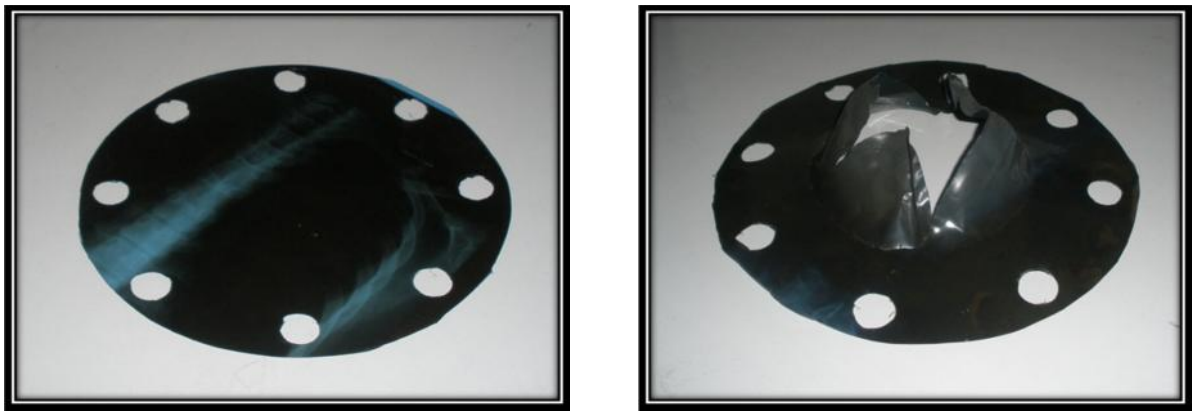

***Figure7.16: Condition of X-ray Diaphragm before and after Shock Wave generation***

**7.6.2 REXINE:** The Rexine Diaphragm takes less pressure about 4kg/cm$^2$ and MACH number less than X-RAY film. And the rupture of the Diaphragm does not uniform like X-ray film, it is divided into two portions in the middle section. The rupturing condition of the Rexine is shown in the figure

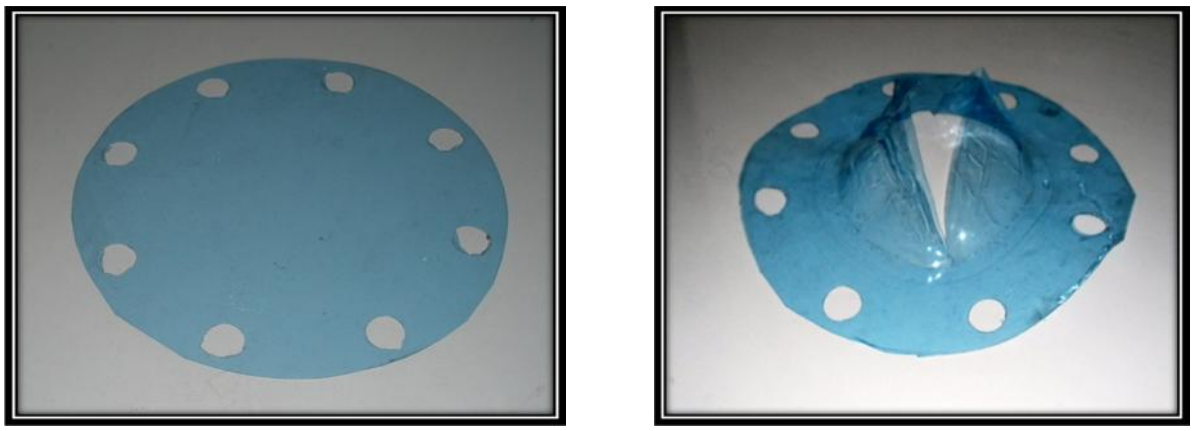

***Figure7.17: Condition of Rexine Diaphragm before and after Shock Wave generation***

**7.6.3 CELLULOID SHEET:** This Diaphragm was totally unsatisfactory. The pressure taken by this is about 3.5 kg/cm$^2$ and Mach number is less then M=1. And the rupture was not uniform, as it is ruptured at the middle only. The rupturing condition of the Celluloid Sheet is shown in the figure9.5

***Figure7.18: Condition of Celluloid Sheet Diaphragm before and after Shock Wave generation***

## 7.6.4 High Pressure Limit and Respective MACH Number of the Diaphragms:

| DIAPHRAGM | PRESSURE Kg/cm$^2$ | MACH NUMBER |
|---|---|---|
| Celluloid Sheet | 3.5 | M<1 |
| Rexine | 4.0 | M≤1 |
| X-ray film | 4.5 | M≈1.2 |

# Conclusion

In the study of Diaphragm characteristics in generation of Shock Wave in the Shock Tube we come to a decision that among the three Diaphragms which one is best to use in the shock tube. In our investigation we select three kinds of celluloid which are available in market. After selection we performed several material tests to know the material properties of the diaphragms. In hardness test we used Rockwell Hardness test, in which the Rexine gave best hardness and then X-ray film and less hardness was shown by the celluloid sheet. For the determination of the ultimate tensile strength we used Universal Material Testing Machine. In the ultimate tensile strength the X-ray film shows best tensile strength among three materials. Rexine shows little less tensile strength than X-ray film, and celluloid sheet's tensile strength was unsatisfactory. After measuring material properties we performed the shock tube test. The Shock Tube we used was open atmosphere type and microsecond level time measuring device is used to measure the wave propagation time. After performing shock tube test we observed that plastic celluloid sheet was so unsatisfactory for generation of shock as the Mach number <1. The Rexine shows also unsatisfactory results to generate shock wave, for some experiment it shows Mach number 1 and in some case less than 1. So this could not be suitable for shock tube Diaphragm. The X-ray film shows most satisfactory result in the shock tube. It takes more pressure and Mach number was more than 1, which indicates shock wave is generated.

Therefore we come to a decision that among the three Diaphragms X-ray film is best and suitable for generation of shock wave in the shock tube which is available in the normal markets at cheap price. So for generation of shock wave in shock tube X-ray film can be used.

## Reference

1. Frank M white, fluid Mechanics-Fourth Edition, McGrew Hill Publishers.

2. Edward j. Shaughnessy, Ira M Kats, James P, Schaffer; Introduction to Fluid Mechanics, Oxford University press.

3. Z Jiang K. Takayama H, Babinsky, T Meguro, Transient Shockwave flows in tubes with a sudden change in cross section, Shockwaves(1997) 7:151-162

4. Z Jiang v Wang , Y Miura K. Takayama.Three-Dimensional Propagation of the transmitted Shock wave in a square cross sectional Chamber ,Springer –Verlag 2003,Shock waves (2003) 13:103-111

5. Tsukaa Irie, Tsuyoshi Yasunobu, Hideo kashimura, Toshaiki Setoguchi, Kazayasu matsuo, characteristics of Spherical Shock Wave and circulars pulse Jet Generated by discharge of propagating Shockwave at open end of tube of thermal Science .Vol .12 no.3.

6. Doig, G.C., Barber, T.J., Leonard, E., Neely, J., Kleine, H., 2008. Methods for investigating supersonic ground effect in a blowdown wind tunnel, Shock Waves, 18: 155-15.

7. Kobiera, A., Szymczyk, J., Wola'nski, P., Kuhl, A., 2009. Study of the shockinduced acceleration of hexane droplets, Shock Waves, 18: 475-85.

8. Pianthong, K., Zakrzewski, S., Behnia, M., Milton, B.E., 2002. Supersonic liquid jets: Their generation and shock wave characteristics, Shock Waves, 11: 457-66.

9. Explosion Waves and Shock Waves. VI. The Disturbance Produced by Bursting Diaphragms with Compressed Air .William Payman and Wilfred Charles Furness Shepherd

10. Ref: http://www.plint.co.uk/at2/leaflet/te76.htm

11. Ref: http://www.mee-inc.com/microhar.html

12.Influence of the diaphragm on the metrological characteristics of a shock tube J. N. de Souza Vianna, A. B. de Sousa Oliveiraand J. P. Damion

13. Smith, William F.; Hashemi, Javad (2001), Foundations of Material Science and Engineering (4th ed.), McGraw-Hill, p. 229, ISBN 0-07-295358-6

14. E.L. Tobolski & A. Fee, "Macroindentation Hardness Testing," ASM Handbook, Volume 8: Mechanical Testing and Evaluation, ASM International, 2000, p 203-211, ISBN 0-87170-389-0.